An American National Standard

IEEE Standard Test Procedures for Semiconductor X-Ray Energy Spectrometers

Sponsor
Nuclear Instruments and Detectors Committee
of the
IEEE Nuclear and Plasma Sciences Society

Secretariat

Institute of Electrical and Electronic Engineers, Inc

Approved December 17, 1981
Reaffirmed September 28, 1990

IEEE Standards Board

Approved June 14, 1982
Reaffirmed February 27, 1991

American National Standards Institute

© Copyright 1984 by

The Institute of Electrical and Electronics Engineers, Inc

345 East 47th Street, New York, NY 10017, USA

No part of this publication may be reproduced in any form, in an electronic retrieval system or otherwise, without the prior written permission of the publisher.

Copyright The Institute of Electrical and Electronics Engineers, Inc.
Provided by IHS under license with IEEE
No reproduction or networking permitted without license from IHS
Not for Resale

IEEE Standards documents are developed within the Technical Committees of the IEEE Societies and the Standards Coordinating Committees of the IEEE Standards Board. Members of the committees serve voluntarily and without compensation. They are not necessarily members of the institute. The standards developed within IEEE represent a consensus of the broad expertise on the subject within the Institute as well as those activities outside of IEEE which have expressed an interest in participating in the development of the standard.

Use of an IEEE Standard is wholly voluntary. The existence of an IEEE Standard does not imply that there are no other ways to produce, test, measure, purchase, market, or provide other goods and services related to the scope of the IEEE Standard. Furthermore, the viewpoint expressed at the time a standard is approved and issued is subject to change brought about through developments in the state of the art and comments received from users of the standard. Every IEEE Standard is subjected to review at least once every five years for revision or reaffirmation. When a document is more than five years old, and has not been reaffirmed, it is reasonable to conclude that its contents, although still of some value, do not wholly reflect the present state of the art. Users are cautioned to check to determine that they have the latest edition of any IEEE Standard.

Comments for revision of IEEE Standards are welcome from any interested party, regardless of membership affiliation with IEEE. Suggestions for changes in documents should be in the form of a proposed change of text, together with appropriate supporting comments.

Interpretations: Occasionally questions may arise regarding the meaning of portions of standards as they relate to specific applications. When the need for interpretations is brought to the attention of IEEE, the Institute will initiate action to prepare appropriate responses. Since IEEE Standards represent a consensus of all concerned interests, it is important to ensure that any interpretation has also received the concurrence of a balance of interests. For this reason IEEE and the members of its technical committees are not able to provide a instant response to interpretation requests except in those cases where the matter has previously received formal consideration.

Comments on standards and requests for interpretations should be addressed to:

Secretary, IEEE Standards Board
345 East 47th Street
New York, NY 10017
USA

Copyright The Institute of Electrical and Electronics Engineers, Inc.
Provided by IHS under license with IEEE
No reproduction or networking permitted without license from IHS
Not for Resale

Foreword

(This Foreword is not a part of ANSI/IEEE Std 759-1984, IEEE Standard Test Procedures for Semiconductor Energy X-Ray Spectrometers.)

This document presents standard test procedures for semiconductor X-ray energy spectrometers. Such systems consist of a semiconductor radiation detector assembly and signal processing electronics interfaced to a pulse height analyzer/computer. Companion documents are ANSI/IEEE Std 300-1982, IEEE Standard Test Procedures for Semiconductor Charged-Particle Detectors, ANSI/IEEE Std 301-1976, IEEE Standard Test Procedures for Amplifiers and Preamplifiers for Semiconductor Radiation Detectors for Ionizing Radiation, and ANSI/IEEE Std 325-1971, IEEE Standard Test Procedures for Germanium Gamma-Ray Detectors.

When this standard was approved, the Nuclear Instruments and Detectors Committee of the IEEE Nuclear and Plasma Sciences Society had the following membership:

David C. Cook, *Chair*
Louis Costrell, *Secretary*

J. A. Coleman	T. R. Kohler	P. L. Phelps, Jr
J. F. Detko	H. W. Kraner	J. H. Trainor
F. S. Goulding	W. W. Managan	S. Wagner
F. A. Kirsten	G. L. Miller	F. J. Walter
	D. E. Persyk	

F. John Walter served as project leader for the development of this standard.

At the time it approved this standard, the American National Standards Committee N42 on Radiation Instrumentation had the following personnel:

Louis Costrell, *Chair*
David C. Cook, *Secretary*

American Chemical Society
American Conference of Governmental Industrial Hygienists ..... Jesse Lieberman
American Industrial Hygiene Association
American Nuclear Society ..... F. W. Manning
American Society of Mechanical Engineers
American Society of Safety Engineers
Atomic Industrial Forum
Health Physics Society ..... J. B. Homer Kuper
J. M. Selby *Alt*
Institute of Electrical and Electronics Engineers ..... Louis Costrell
D. C. Cook *Alt*
A. J. Spurgin *Alt*
J. Forster *Alt*
Instrument Society of America ..... M. T. Slind
J. E. Kaveckis *Alt*
Lawrence Berkeley Laboratory ..... L. J. Wagner
Oak Ridge National Laboratory ..... Frank W. Manning
D. J. Knowles *Alt*
US Nuclear Regulatory Commission ..... Robert A. Purple
US Department of Energy ..... Gerald Goldstein
US Department of the Army, Materiel Command ..... Abraham E. Cohen
US Department of the Army, Office of Civil Defense Mobilization ..... Carl R. Siebentritt, Jr

Copyright The Institute of Electrical and Electronics Engineers, Inc.
Provided by IHS under license with IEEE
No reproduction or networking permitted without license from IHS
Not for Resale

US Department of Commerce, National Bureau of Standards ..... Louis Costrell
US Naval Research Laboratory ..... D. C. Cook
Members-at-Large ..... J. G. Bellian
O. W. Bilharz, Jr
John M. Gallagher, Jr
Voss A. Moore
R. F. Shea
E. J. Vallario

When the IEEE Standards Board approved this standard on December 17, 1981, it had the following membership:

Irvin N. Howell, Jr, *Chair*
Irving Kolodny, *Vice Chair*
Sava I. Sherr, *Secretary*

G. Y. R. Allen
J. J. Archambault
James H. Beall
John T. Boettger
Edward Chelotti
Edward J. Cohen
Len S. Corey
Jay Forster
Kurt Greene
Loering M. Johnson
Joseph L. Koepfinger
J. E. May
Donald T. Michael*
J. P. Riganati
Frank Rosa
R. W. Seelbach
Jay A. Stewart
William E. Vannah
Virginius M. Vaughan, Jr
Art Wall
Robert E. Weiler

*Member emeritus

Copyright The Institute of Electrical and Electronics Engineers, Inc.
Provided by IHS under license with IEEE
No reproduction or networking permitted without license from IHS
Not for Resale

CLAUSE PAGE

1. Scope 1

2. References 1

3. Glossary 2

4. Symbols 6

5. Introduction 10

5.1 Detector System 10
5.2 Statistical Limit of Resolution 11
5.3 Preamplifier Noise 12
5.4 Detector Noise 14
5.5 Charge Loss 15
5.6 Electronic Stability and Extraneous Noise 15
5.7 Count-Rate Effects 15
5.8 Detector Material Selection: Germanium Versus Silicon 16
5.9 Detector Efficiency 17
5.10 Resolution of Adjacent Lines and Line-to-Background Ratio 18
5.11 Miscellaneous Other Effects 19

6. General 19

6.1 Definition of Semiconductor X-Ray Energy Spectrometer 19
6.2 General Precautions and Specifications 19
6.3 Simulating the Signal Pulse of a Detector 20

7. Energy Resolution and Spectral Distortion 22

7.1 Noise Measurement by Pulse-Height Distribution (Preferred Method) 22
7.2 Alternate Techniques For Noise Measurement 23
7.3 Noise Linewidth as a Function of Amplifier Time Constants 24
7.4 X-Ray Linewidth Measurements by Pulse Height Distribution 24
7.5 Peak-to-Valley and Peak-to-Tail Ratios 27

8. Pulse Height Linearity 28

8.1 System X-Ray Linearity by Pulse-Height Analyzer Method (Preferred Method) 28
8.2 Integral Linearity by the Bridge Method 28

9. Count Rate Effects 29

9.1 Experimental Arrangement 29
9.2 Pulse-Height Distribution Peak Shift 31
9.3 Spectral Resolution and Line Shape Versus Count Rate 31
9.4 Counting Losses 31

10. Overload Effects 34

10.1 General 34
10.2 Amplifier Gain Recovery Time 34

Copyright The Institute of Electrical and Electronics Engineers, Inc.
Provided by IHS under license with IEEE
No reproduction or networking permitted without license from IHS
Not for Resale

CLAUSE PAGE

11. Pulse Height Stability....35

11.1 Line Voltage Variations 35
11.2 Temperature Effects 36
11.3 Gain Stability 36

12. Efficiency 36

12.1 Window Attenuation Measurements with Glass Fluorescent Source (Preferred Method for Instruments Intended for Use Below 5 keV) 37
12.2 Window Attenuation Measurement with Radioactive Sources 43
12.3 High Energy Efficiency Measurements 44

13. Bibliography....46

Copyright The Institute of Electrical and Electronics Engineers, Inc.
Provided by IHS under license with IEEE
No reproduction or networking permitted without license from IHS Not for Resale

An American National Standard

IEEE Standard Test Procedures for Semiconductor X-Ray Energy Spectrometers

1. Scope

This document presents standard test procedures for semiconductor X-ray energy spectrometers. Such systems consist of a semiconductor radiation detector assembly and signal processing electronics interfaced to a pulse height analyzer/computer. Test procedures for pulse-height analyzers and computers are not covered in this document. Section 5. is essentially tutorial.

This standard is not intended to imply that all tests described herein are mandatory, but only that such tests as are carried out shall be performed in accordance with the procedures described herein.

Companion documents to this standard are ANSI/IEEE Std 300-1982 [1],[1] ANSI/IEEE Std 301-1976 [2], and ANSI/IEEE Std 325-1971 [3].

The list of symbols and the glossary were derived from those in the companion documents.

Contrary to previous convention in the X-ray spectroscopy field, this document utilizes the characteristic energy E of the X-ray rather than its wavelength λ. This approach is consistent with the fact that the basic quantity measured by this type of spectrometer is the X-ray energy. A convenient conversion is provided by the relationship

$$\lambda(\text{m}) = 12.4 \cdot 10^{-10} E^{-1}(\text{keV})$$

$$\lambda(A^0) = 12.4 E^{-1} \text{ (keV)}$$

2. References

[1] ANSI/IEEE Std 300-1982, IEEE Standard Test Procedures for Semiconductor Charged-Particle Detectors.

[2] ANSI/IEEE Std 301-1976, IEEE Standard Test Procedures for Amplifiers and Preamplifiers for Semiconductor Radiation Detectors for Ionizing Radiation.

[3] ANSI/IEEE Std 325-1971, IEEE Standard Test Procedures for Germanium Gamma-Ray Detectors.

[4] IEC Publication 333 (1983), Test Procedures for Semiconductor Detectors.[2]

[1]The numbers in brackets correspond to those of the references listed in Section 2.
[2]IEC Standards are available in the US from American National Standards Institute, 1430 Broadway, New York, NY 10018

Copyright © 1984 IEEE All Rights Reserved

Copyright The Institute of Electrical and Electronics Engineers, Inc.
Provided by IHS under license with IEEE
No reproduction or networking permitted without license from IHS
Not for Resale

[5] IEC Publication 340 (1979) (Second Edition), Test Procedures for Amplifiers and Peamplifiers for Semiconductor Detectors for Ionizing Radiation.

[6] IEC Publication 430 (1973), Test Procedures for Germanium Gamma-Ray Detectors.

3. Glossary

analog-to-digital converter (adc): A device whose input is information in analog form and whose output is the same information in digital form.

background (associated with a spectral peak from a semiconductor detector): Non-ideal spectral response which results from radiation which is not a part of the monoenergetic line of interest.

baseline (at pulse peak): The instantaneous value that the voltage would have had at the time of the pulse peak in the absence of that pulse.

baseline restoration (BLR): Appropriate linear or non-linear technique(s), or their combination, used to accelerate the return of a voltage to its baseline.

bias (of a semiconductor radiation detector): The voltage applied to a detector to produce the electric field to sweep out the signal charge.

biased amplifier: An amplifier giving essentially zero output for all inputs below a threshold and having constant incremental gain for all inputs above the threshold up to a specified maximum amplitude.

bias resistor (of a semiconductor radiation detector): The resistor through which bias voltage is applied to a detector.

breakdown (of a semiconductor diode): A phenomenon occurring in a reverse biased semiconductor diode, the initiation of which is observed as a transition from a region of high dynamic resistance to a region of substantially lower dynamic resistance for increasing magnitude of reverse current.

breakdown region (of a semiconductor diode characteristic): That entire region of the voltagecurrent characteristic beyond the initiation of breakdown for increasing magnitude of reverse current.

breakdown voltage (of a semiconductor diode): The voltage measured at a specified current in the breakdown region.

capacitance (of a semiconductor radiation detector): The small-signal capacitance measured between terminals of the detector under specified conditions of bias and frequency.

charge carrier (of a semiconductor): A mobile conduction electron or mobile hole.

charge collection time (of a semiconductor radiation detector): The time interval, after the passage of an ionizing particle, for the integrated current flowing between the terminals of the detector to increase from 10% to 90% of its final value.

clip, clipping (jargon): A limiting operation such as 1) use of a high-pass filter (see **differentiated**), or 2) a nonlinear operation such as diode limiting of pulse amplitude.

crest factor (semiconductor radiation detectors) (of an average reading or root-mean-square voltmeter): The ratio of the peak voltage value that an average reading or root-mean-square voltmeter will accept without overloading to the full-scale value of the range being used for measurement.

***cr-rc* shaping:** The pulse shaping present in an amplifier that has a simple high-pass filter consisting of a capacitor and a resistor together with a simple, low-pass filter, separated by impedance isolation. Pulse shaping in such an amplifier cuts off at 6 decibels per octave at both ends of the band.

dc level: See **baseline.**

Copyright © 1984 IEEE All Rights Reserved

Copyright The Institute of Electrical and Electronics Engineers, Inc.
Provided by IHS under license with IEEE
No reproduction or networking permitted without license from IHS Not for Resale

dead layer thickness (of a semiconductor radiation detector): The thickness of an inactive region (in the form of a layer) through which incident radiation must pass to reach the sensitive volume.

decay time constant: The time for a true single exponential waveform to decay to a value of $1/e$ of the original height.

depletion layer (region) (in a semiconductor): A region in which the charge-carrier charge density is insufficient to neutralize the net fixed charge density of donors and acceptors. In a diode-type semiconductor radiation detector the depletion region is the sensitive region of the device.

detector geometry (detector jargon): The physical configuration of a solid-state detector.

differentiated (pulse) (pulse amplifier jargon): A pulse is *differentiated* when it is passed through a high-pass network, such as a *CR* filter.

efficiency (of a semiconductor radiation detector for a monoenergetic radiation source): The ratio of the number of events in the spectral distribution to the total number of photons incident on the active detector volume during the same time interval.

energy resolution (FWHM) (of a semiconductor radiation detector): The detector's contribution (including detector leakage current noise), expressed in units of energy, to the FWHM of a pulse-height distribution corresponding to an energy spectrum.

energy resolution (percent) (of a semiconductor radiation detector): One hundred times the energy resolution divided by the energy for which the resolution is specified.

equivalent noise referred to input (of a linear amplifier): The value of noise at the input that would produce the same value of noise at the output as does the actual noise source.

full energy peak (for a monoenergetic photon spectrum for a semiconductor spectrometer system): The distribution of events within the peak of the pulse-height distribution spectrum representing response to the monoenergetic photon source.

NOTE — Notwithstanding other definitions or procedures for subtracting background and other distortions, the full energy peak intensity is defined as not including any events which exceed a Gaussian distribution by more than a factor of two σ.

full energy peak efficiency (of a semiconductor radiation detector): The ratio of the number of events in the full energy peak of the spectral distribution to the total number of photons incident on the active detector volume during the same time interval.

full width at fiftieth maximum: Same as FWHM except that measurement is made at one fiftieth of the maximum ordinate rather than one half.

full width at half maximum: The full width of a distribution measured at half the maximum ordinate. For a normal distribution, it is equal to $2(2\ ln\ 2)^{1/2}$ times the standard deviation σ.

full width at tenth maximum: Same as FWHM except measurement is made at one tenth of the maximum ordinate rather than one half.

FWFM: (See **full width at fiftieth maximum.)**

FWHM: (See **full width at half maximum.)**

FWTM: (See **full width at tenth maximum.)**

gate: A device or element that, depending upon one or more specified inputs, has the ability to permit or inhibit the passage of a signal.

inactive region (of a semiconductor radiation detector): A region of a detector in which charge created by ionizing radiation does not contribute significantly to the signal charge.

integral nonlinearity (INL) (of a pulse amplifying system): The maximum nonlinearity (deviation) over the specified operating range of a system, usually expressed as a percentage of the maximum of the specified range.

integrated (pulse) (pulse amplifier jargon): A pulse is *integrated* when it is passed through a low-pass network, such as a single *RC* network or a cascaded *RC* network.

Copyright © 1984 IEEE All Rights Reserved

Copyright The Institute of Electrical and Electronics Engineers, Inc.
Provided by IHS under license with IEEE
No reproduction or networking permitted without license from IHS Not for Resale

integrating preamplifier: A pulse preamplifier in which individual pulses are intentionally integrated by passive or active circuits.

intrinsic semiconductor: A semiconductor containing an equal number of free holes and electrons throughout its volume.

junction (of a semiconductor radiation detector): A region of transition between semiconductor regions of different electrical properties, (for example, n-n^+, p-n, p-p^+ semiconductors), or between a metal and a semiconductor.

junction depth (of a *p-n*semiconductor radiation detector): The distance below the crystal surface at which the conductivity type changes.

leakage current (of a semiconductor radiation detector): The total detector current flowing at the operating bias in the absence of radiation.

linear gate: A gate whose presence does not affect the linearity of the gated signal.

line-to-background ratio (of a spectral line): The ratio of the intensity of a monoenergetic line to the intensity of the background immediately adjacent to the line.

lithium-drifted detector: A detector made by the lithium compensation process.

lithium drifting: A technique for compensating p-type material by causing lithium ions to move through a crystal under an applied electric field in such a way as to compensate the charge of the bound acceptor impurities.

load impedance (of a semiconductor radiation detector): The impedance shunting the detector, and across which the detector output voltage signal is developed.

load resistance (of a semiconductor radiation detector): The resistive component of the load impedance.

MCA: Multichannel analyzer.

modal channel: The modal channel is that channel in the distribution containing the largest number of counts.

multichannel analyzer (MCA): An instrument which digitizes analog amplitude signal pulses and stores them in a memory as a function of theft analog amplitude.

noise linewidth.: The contribution of noise to the width of a spectral peak.

noninjecting contact (of a semiconductor radiation detector).: A contact at which the carrier density in the adjacent semiconductor material is not changed from its equilibrium value.

nonlinearity (of a pulse amplifying system): Distortion caused by a deviation from a desired linear relationship between specified measures of the output and input pulse amplitudes of a system or device.

ohmic contact (of a semiconductor radiation detector): A purely resistive contact, that is, one that has a linear voltage-current characteristic throughout its entire operating range.

overload pulse: Any signal that drives a section of the amplifying chain into saturation.

paralyzable system: Any system or device whose response characteristics contain a region where the ratio of output-to-input count rate decreases with increasing input count rate.

partially dead region or layer (of a semiconductor detector): Any region or layer on or in the detector which contributes an output pulse which is less than the full energy peak for that incident radiation.

percent energy resolution: (See energy resolution.)

pile-up (of signal pulses): Two pulses (signals) are said to be piled-up when a second pulse occurs before the transient response of the preceding pulse has decayed to a negligible value.

pile-up rejection: A technique used to identify and reject pulses (signals) that are piled up.

***p-i-n* detector:** A detector consisting of an intrinsic or nearly intrinsic region between a p and n region.

Copyright © 1984 IEEE All Rights Reserved

Copyright The Institute of Electrical and Electronics Engineers, Inc.
Provided by IHS under license with IEEE
No reproduction or networking permitted without license from IHS Not for Resale

pole-zero cancellation (PZ): A technique used to cancel out the effects of a singularity in an amplifiers' transfer function in order to affect a monotonic return of signal pulses to the baseline.

pulse decay time (t_d): The interval between the instants at which the instantaneous value last reaches specified upper and lower limits, namely, 90% and 10% of the peak pulse value unless otherwise stated. (In the case of a step function applied to an amplifier that has simple *CR-RC* shaping, the decay time is given by $t_d = 3.36\ CR$.)

pulse rise time (t_r): The interval between the instants at which the instantaneous value first reaches specified lower and upper limits, namely, 10% and 90% of the peak pulse value unless otherwise specified. (In the case of a step function applied to an RC low-pass filter, the rise time is given by $t_r = 2.2\ RC$. In the case of a step function applied to an amplifier that has simple *CR-RC* shaping, that is, one high-pass and one low-pass *RC* filter of equal time constants, the rise time is given by $t_r = 0.57\ RC$.)

punch-through voltage (of a semiconductor radiation detector): The voltage at which a junction detector becomes fully depleted.

resolution, energy (percent): (See **energy resolution [percent].**)

SCA: Single-channel analyzer,

semiconductor, compensated: A semiconductor in which one type of impurity or imperfection (for example, donor) partially cancels the electric effects of the other type of impurity or imperfection (for example, acceptor).

semiconductor radiation detector: A semiconductor device that utilizes the production and motion of excess free charge carriers for the detection and measurement of incident radiation.

space-charge generation (in a semiconductor radiation detector): The thermal generation of free charge carriers in the space-charge region.

space-charge region (of a semiconductor radiation detector): A region in which the net charge density is significantly different from zero. (See also depletion region.)

spectral line: A sharply peaked portion of the spectrum that represents a specific feature of the incident radiation, usually the full energy of a monoenergetic radiation.

spectrum (radiation): A distribution of the intensity of radiation as a function of energy or its equivalent electric analog (such as charge or voltage) at the output of a radiation detector.

standard source diameter: The diameter of the X-ray emission source which is used to measure the response characteristics of the spectrometer. Unless otherwise specified, this is assumed to be a point source.

standard working axis (of a semiconductor X-ray energy spectrometer): A straight line drawn between the center of the entrance window on the detector and the specified location of the source of X-rays.

surface barrier contact: A rectifying contact that is characterized by a potential barrier associated with an inversion or accumulation layer; said inversion or accumulation layer being caused by surface charge resulting from the presence of surface states and work function differences, or both.

surface barrier radiation detector: A radiation detector for which the principal rectifying junction is a surface barrier contact.

sweep-out time, charge(of a semiconductor radiation detector): (See **charge collection time.**)

tail or tailing (on a monoenergetic peak): Any peak shape distortion that does not comply with the limits defining the full energy peak intensity and that does not come from a source of radiation other than the monoenergetic source in question.

totally depleted detector: A detector in which the thickness of the depletion region is essentially equal to the thickness of the semiconductor material.

transmission detector: A totally depleted detector whose thickness including its entrance and exit windows is sufficiently small to permit radiation to pass completely through the detector.

window (of a semiconductor radiation detector): (See **dead layer thickness.**)

Copyright © 1984 IEEE All Rights Reserved

Copyright The Institute of Electrical and Electronics Engineers, Inc.
Provided by IHS under license with IEEE
No reproduction or networking permitted without license from IHS
Not for Resale

window amplifier: (See **biased amplifier.**)

working distance: The distance, measured along the working axis, between the source of X-rays and the outermost window on the detector.

4. Symbols

Symbol	Term Denoted
A	Intensity of full energy monoenergetic peak; total number of counts in a full energy peak.
A_b	number of counts in the background under a peak.
A_E	intensity of spectral peak at energy E; the total number of counts in the full energy peak of energy E.
A_{Mn}	intensity of backscattered Mn K_α peak.
A_t	Total peak area, number of counts in the full energy peak, plus background.
a, b	constants characterizing noise.
B	bandwidth.
BLR	baseline restorer
C	electrical capacitance.
C_d	detector capacitance.
C_c	calibrated capacitor used to couple a pulse generator to a circuit under test.
C_{eff}	effective input capacitance of a preamplifier.
C_f	feedback capacitance in the integrating loop of a charge-sensitive preamplifier.
C_t	total capacitance at a preamplifier input.
C_1	the average number of counts per channel in five contiguous channels centered around the energy of 5.4 keV in the tail of a Mn K_α X-ray energy spectrum.
C_2	same as C_1 except 4.5 keV.
C_3	same as C_1 except 1 keV.
Δ	FWHM of a monoenergetic spectral peak.
Δ^A_E	FWHM expressed in units of energy, due to amplifier noise.
Δ^A_N	FWHM expressed in channels, due to amplifier noise.
Δ^A_Q	FWHM expressed in units of charge, due to amplifier noise.
Δ^D_E	FWHM expressed in units of energy, due to detector noise.
Δ^D_N	FWHM expressed in channels, due to detector noise.

Copyright © 1984 IEEE All Rights Reserved

Copyright The Institute of Electrical and Electronics Engineers, Inc.
Provided by IHS under license with IEEE
No reproduction or networking permitted without license from IHS
Not for Resale

Symbol	Term Denoted
Δ^{D}_{Q}	FWHM expressed in units of charge, due to detector noise.
ΔE_{Max}	the maximum deviation, in units of energy, between the measured linearity curve and the ideal linear response curve.
Δ_{N}	a shift (expressed in channels) of the peak center (modal) channel.
Δ^{O}_{E}	FWHM, expressed in units of energy, due to all factors other than electrical noise.
Δ^{O}_{N}	FWHM, expressed in channels, due to all factors other than electrical noise.
Δ^{S}_{E}	FWHM for monoenergetic incident radiation, expressed in units of energy, including all spectral broadening effects.
Δ^{S}_{N}	FWHM for monoenergetic incident radiation, expressed in channels, including all spectral broadening effects.
Δ^{T}_{E}	FWHM, expressed in units of energy, due to the combined effect of detector and amplifier noise.
Δ^{T}_{N}	FWHM, expressed in channels, due to the combined effect of detector and amplifier noise.
Δ^{T}_{Q}	FWHM, expressed in units of charge, due to the combined effect of detector and amplifier noise.
E	energy of a particle or photon.
ε	average energy required to form one hole-electron pair in a semiconductor.
e	electron charge or natural log base (2.71828).
E_{F}	the energy corresponding to the maximum linear output of a spectrometer.
e_{ni}	equivalent root-mean-square noise voltage referred to the preamplifier input.
e_{no}	root-mean-square noise voltage.
e_{qi}	root-mean-square noise in units of charge at the amplifier input.
F	Fano Factor, an empirical coefficient that corrects for the fact that Poisson statistics are not obeyed.
G_{B}	gain of a biased amplifier.
ψ	noise spectral power density.
i	detector noise current.
I	electric current.
I_{d}	detector leakage current.
I_{o}	diode equivalent Gaussian noise current in a specified frequency band.

Copyright © 1984 IEEE All Rights Reserved

Copyright The Institute of Electrical and Electronics Engineers, Inc.
Provided by IHS under license with IEEE
No reproduction or networking permitted without license from IHS
Not for Resale

Symbol	Term Denoted
INL	integral nonlinearity; the maximum deviation from linearity expressed as a percentage of the maximum linear output.
k	Boltzmann's constant.
K	constant relating FWHM in units of energy to FWHM in units of charge.
MCA	multichannel analyzer.
L_D	differential nonlinearity of an amplifier.
L_i	integral nonlinearity of a biased amplifier.
L_I	integral nonlinearity of an amplifier.
N	channel number corresponding to the maximum of a monoenergetic spectral peak.
N_{avg}	average number of counts in all channels of a multichannel pulse-height analyzer spectrum.
N_B	equivalent number of channels suppressed by a biased amplifier.
N_p	the total number of counts in the modal (peak center) channel of the Mn full energy peak from a Mn *K* X-ray energy spectrum.
N_x	number of counts in channel *X* of a multichannel pulse-height analyzer spectrum.
P_1	the peak-to-tail ratio at 5.4 keV for a Mn *K* X-ray energy spectrum.
P_2	the peak-to-tail ratio at 4.5 keV for a Mn *K* X-ray energy spectrum.
P_3	the peak-to-tail ratio at 1 keV for a Mn *K* X-ray energy spectrum.
PZ	pole-zero cancellation.
Q	electric charge.
R	electrical resistance.
R_c	resistor used in parallel with C_c to effect pole-zero cancellation.
R_f	a resistor in parallel with C_f (used to stabilize the operating point of the first active element in a preamplifier).
r_i	input data rate to a system or device.
R_L	detector load resistor.
r_0	output data rate of a system or device.
S_L	output pulse height stability.
S_M	sensitivity of mca or adc/computer system expressed in energy units of eV/channel.
T	absolute temperature.

Copyright © 1984 IEEE All Rights Reserved

Copyright The Institute of Electrical and Electronics Engineers, Inc.
Provided by IHS under license with IEEE
No reproduction or networking permitted without license from IHS
Not for Resale

Symbol	Term Denoted
t_c	charge collection time in a detector.
t_d	dead time in a device or system.
t_e	observed detector rise time due to the combined effects of the charge collection time and detector electrical rise time.
t_p	detector electrical rise time.
t_r	rise time (10% to 90%).
τ	time constant.
τ_c	time constant of a *CR* network used to simulate the rise of a pulse from a radiation detector.
τ_d	decay time constant.
t_w	width of a pulse, in time units, at the baseline established by the discriminator threshold level.
V	electric voltage.
V_a	amplitude of amplifier output voltage.
V_d	detector bias voltage.
V_D	depletion voltage
V_P	amplitude of the voltage step impressed on C_c by the pulse generator.
W_E	window attenuation index at energy E as determined by spectrum from NBS-SRM 477 excited with ^{55}Fe.
X	channel number in an inca or computer display of a photon energy spectrum.
Z	atomic number
Z_0	characteristic impedance
λ	the characteristic wavelength associated with an X-ray photon.
δ^S_E	FWTM for monoenergetic incident radiation, expressed in units of energy, including all spectral broadening effects.
δ^S_N	FWTM for monoenergetic incident radiation, expressed in channels, including all spectral broadening effects.
δ^T_E	FWTM, expressed in units of energy, due to the combined effect of detector and amplifier noise.
δ^O_E	FWTM, expressed in units of energy, due to all factors other than electrical noise.
δ^T_N	FWTM, expressed in channels, due to the combined effects of detector and amplifier noise.

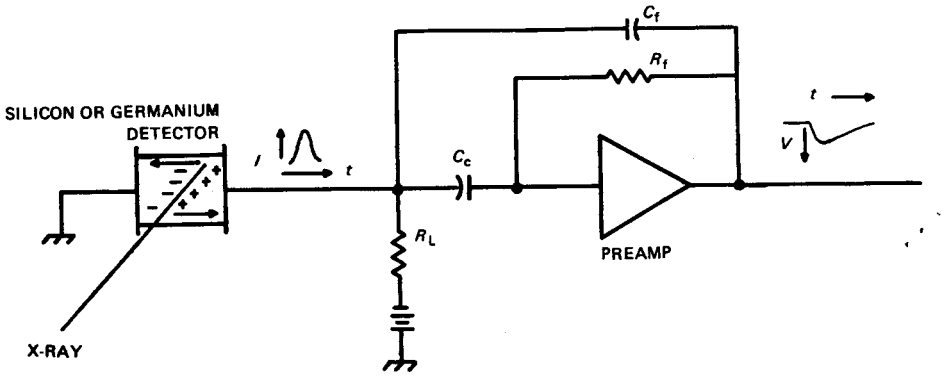
Copyright © 1984 IEEE All Rights Reserved

Copyright The Institute of Electrical and Electronics Engineers, Inc.
Provided by IHS under license with IEEE
No reproduction or networking permitted without license from IHS
Not for Resale

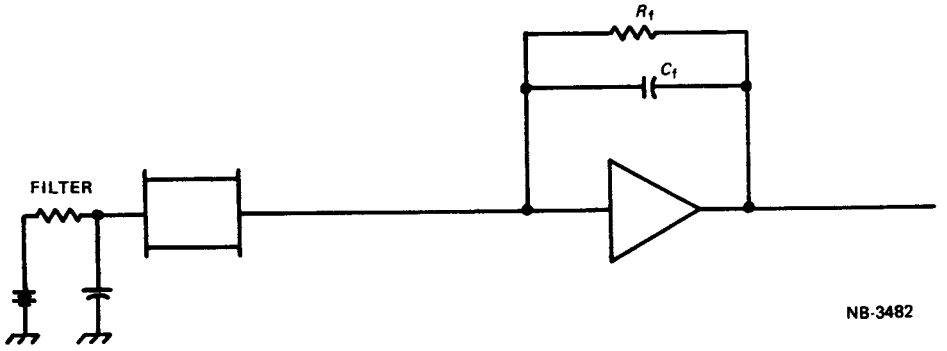
5. Introduction

5.1 Detector System

A semiconductor detector is analogous to a gas ion chamber in which the gas has been replaced by a solid. Figure 1 illustrates this type of detector and its preamplifier configuration. The detector consists of a semiconducting crystal between two conducting electrodes. A potential difference is established between the electrodes thereby producing an electric field in the semiconductor. When an X-ray photon enters the semiconductor it produces free charge carriers in the crystal, the number of which is proportional to the energy lost by the X-ray photon. The charge motion resulting from the influence of the electric field produces an induced current pulse in the external circuit. This current represents the basic signal information, and the integrated current pulse is proportional to the energy lost by the X-ray. The pulses are routed to a multichannel pulse-height analyzer (MCA) where they are sorted and stored according to the amplitude distribution to produce a pulse-height spectrum that corresponds to the X-ray energy spectrum. The MCA may be a dedicated instrument or an analog-to-digital converter (adc) interfaced to a computer.



(a) ac-Coupled Configuration



(b) dc-Coupled Configuration

Figure 1—Schematic of Semiconductor Detector and Preamplifier

The semiconductor materials most frequently used for X-ray spectrometers, silicon and germanium, do not have sufficiently high resistivity to withstand large electric fields without excessive leakage currents. It is therefore necessary to use special techniques to limit the current flow through the semiconductor device. This is usually accomplished by utilizing the space charge region of a reverse biased diode junction as the detector-sensitive volume. Silicon and germanium are the only semiconductor materials presently available with sufficient crystalline perfection

Copyright © 1984 IEEE All Rights Reserved

Copyright The Institute of Electrical and Electronics Engineers, Inc.
Provided by IHS under license with IEEE
No reproduction or networking permitted without license from IHS Not for Resale

and purity to be generally useful for this type of device, although work is continuing on other semiconductors such as HgI_2, CdTe, and GaAs. Although both silicon and germanium crystals are available in very pure form, the electrically active impurity level is sometimes too high to allow fabrication of usefully large detectors. This limitation can be overcome by using mobile lithium ions to compensate the electrically active impurities. If the lithium compensation technique is used, the germanium semiconductor device is subject to inherent stability problems since the compensation can be classed as highly unstable at room temperature and therefore lithium-compensated germanium devices must be stored at reduced temperatures. In silicon the compensation is quasi-stable, with the degree of stability depending on the presence of other impurities in the crystal and on the details of the device fabrication.

Since there is no internal gain in the type of semiconductor detector considered here, the problem of noise in the detector and in the preamplifier circuits is significant, particularly at low X-ray energies. Consequently, both the semiconductor detector and first stage of the preamplifier are usually operated at low temperature to reduce the thermal noise.

Energy resolution is one of the most important characteristics of an X-ray energy spectrometer since it sets the limit on the ability to resolve closely spaced lines. Figure 2 shows the separation of adjacent elements as a function of atomic number.

In comparing instruments it is necessary also to examine the other specifications, since improved energy resolution may be provided at the expense of other important parameters such as count-rate capability, gain stability, and detector size (efficiency).

The limit resulting from the statistical uncertainty involved in the process whereby the incident X-ray energy produces free charge carriers is a fundamental limit on energy resolution and is discussed in detail in 5.2. Preamplifier noise and detector noise also affect the resolution and are examined in 5.3 and 5.4, respectively. Charge loss from trapping and recombination can also have significant effects on the spectral quality. The peak-width broadening from charge loss typically increases with increasing energy since the fluctuation in the amount of charge trapped usually increases with total charge. *Partially dead* regions or layers can also produce spectral distortion in the form of low-energy tails, nonlinearities, and loss of detector efficiency at low energies. These effects are described in 5.5.

Electronic stability is an important variable that includes not only the stability of the preamplifier, but also that of other parts of the system, such as the main amplifier and MCA.

Effects of high count rate such as pulse pile-up and dc level shifts are also important. Every time an event produces a pulse in the amplifying equipment, the dc levels throughout the system are perturbed and take some time to return to their original values. If another event occurs within this time interval, its effective output pulse height may be altered, thereby contributing to spectral distortion.

5.2 Statistical Limit of Resolution

If Poisson (random) statistics are applied to the process of the X-ray energy loss mechanism by free charge carrier formation, it is possible to calculate the statistical broadening of a monoenergetic X-ray peak from

$$\text{FWHM} = 2.35\sqrt{\varepsilon E}$$

where

E = energy of the incident radiation
ε = average energy required to create a free electron-hole pair

Frequently used values of ε at 77 K are 3.8 eV/pair for silicon and 3.0 eV/pair for germanium. In fact, the charge production process does not follow Poisson statistics because the multiple events that occur in the energy loss process

Copyright © 1984 IEEE All Rights Reserved

Copyright The Institute of Electrical and Electronics Engineers, Inc.
Provided by IHS under license with IEEE
No reproduction or networking permitted without license from IHS Not for Resale

are correlated. Therefore, the statistical formula is usually modified by inserting a correction factor F (called the Fano Factor), resulting in the expression $\text{FWHM} = 2.35\sqrt{\varepsilon E}$. This corrects for the fact that the observed broadening is substantially less than predicted by Poisson statistics. For silicon and germanium, F is not accurately known, but measurements have indicated limits between 0.05 and 0.15.

Since it is not possible to measure the Fano Factor and the resolution broadening caused by charge carrier trapping independently, the two effects are frequently combined in the value assumed for F. This is equivalent to the assumption that the charge loss (trapping) is a constant fraction of the free charge created.

5.3 Preamplifier Noise

Preamplifier noise arises from a number of sources. One is the thermal noise in the input field-effect transistor (FET) of the preamplifier (see Fig 1). This is usually minimized by cooling the FET and using selected FETs. With regard to the FET contribution, the signal-to-noise ratio (S/n) decreases with increasing total capacitance at the FET gate and therefore decreases with increasing detector area. Thus, there is an important compromise between detector size and the observed S/n. Parasitic capacitance also affects S/n. Consequently, the physical configuration of the detector and preamplifier package is critical. The resistors R_f and R_L shown in the circuit of Fig 1(a) also can be important sources of noise. In order to minimize the effect of stray capacitance and resistor noise, C_c and R_L are usually eliminated by dc coupling the detector to the gate of the first FET as in Fig 1(b). Hence all of the current caused by the radiation must flow through R_f or the high impedance gate of the field effect transistor. This can change the FET operating point and the overall gain of the system, unless there is sufficient dc feedback via R_f to provide the required count rate versus gain stability. The greater the feedback resistance (R_f), the smaller the resistor noise contribution, but the poorer the count rate-energy product capability. This presents an important trade-off consideration between noise broadening of the resolution and performance at high count rates. In this respect, it should be pointed out that it is not enough to specify just the simple count-rate capability because it is the product of count rate and average radiation energy that is important, for example, 100 keV X-rays present 20 times the count-rate problem of 5 keV X-rays. Other more sophisticated feedback mechanisms such as optical feedback, dc feedback, or pulsed optical feedback can be used in place of R_f and are in common usage as a method for reducing noise. However, these techniques also involve similar resolution versus count-rate compromises.

Copyright © 1984 IEEE All Rights Reserved

Copyright The Institute of Electrical and Electronics Engineers, Inc.
Provided by IHS under license with IEEE
No reproduction or networking permitted without license from IHS Not for Resale

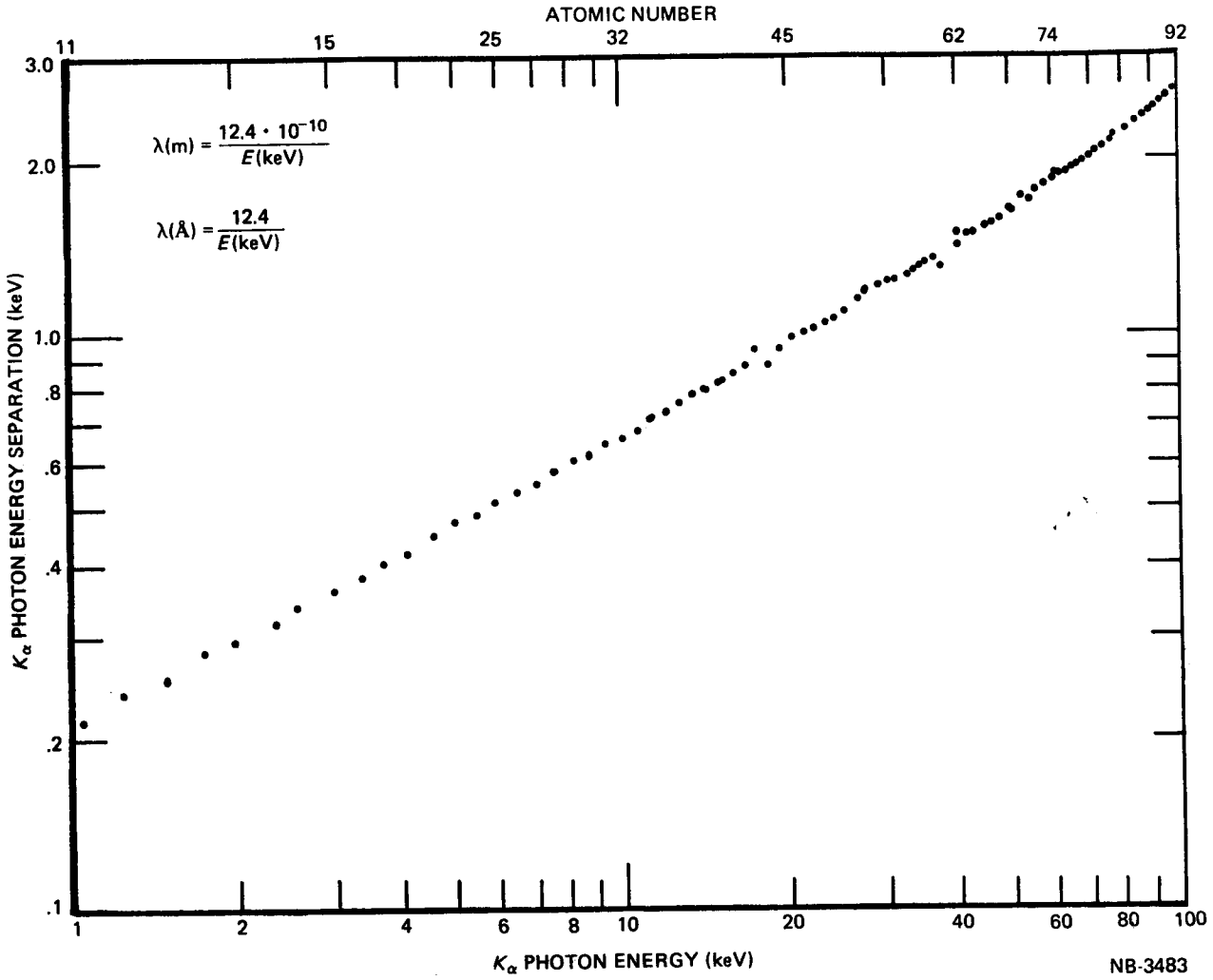


Figure 2—Spectral Line Separation as a Function of Energy and Atomic Number

Figure 3 shows the combined effects of preamplifier noise and statistics for two values of Fano Factor, preamplifier noise and ε. The preamplifier contribution is independent of energy, while the statistical broadening varies as the square root of the energy. At a noise level of about 400 eV, the preamplifier noise dominates the entire range of interest for the *K*-lines of the stable elements, while with 100 eV noise, the noise and statistical effects are about equal at the photon energy of 3.7 keV.

Copyright © 1984 IEEE All Rights Reserved

Copyright The Institute of Electrical and Electronics Engineers, Inc.
Provided by IHS under license with IEEE
No reproduction or networking permitted without license from IHS
Not for Resale

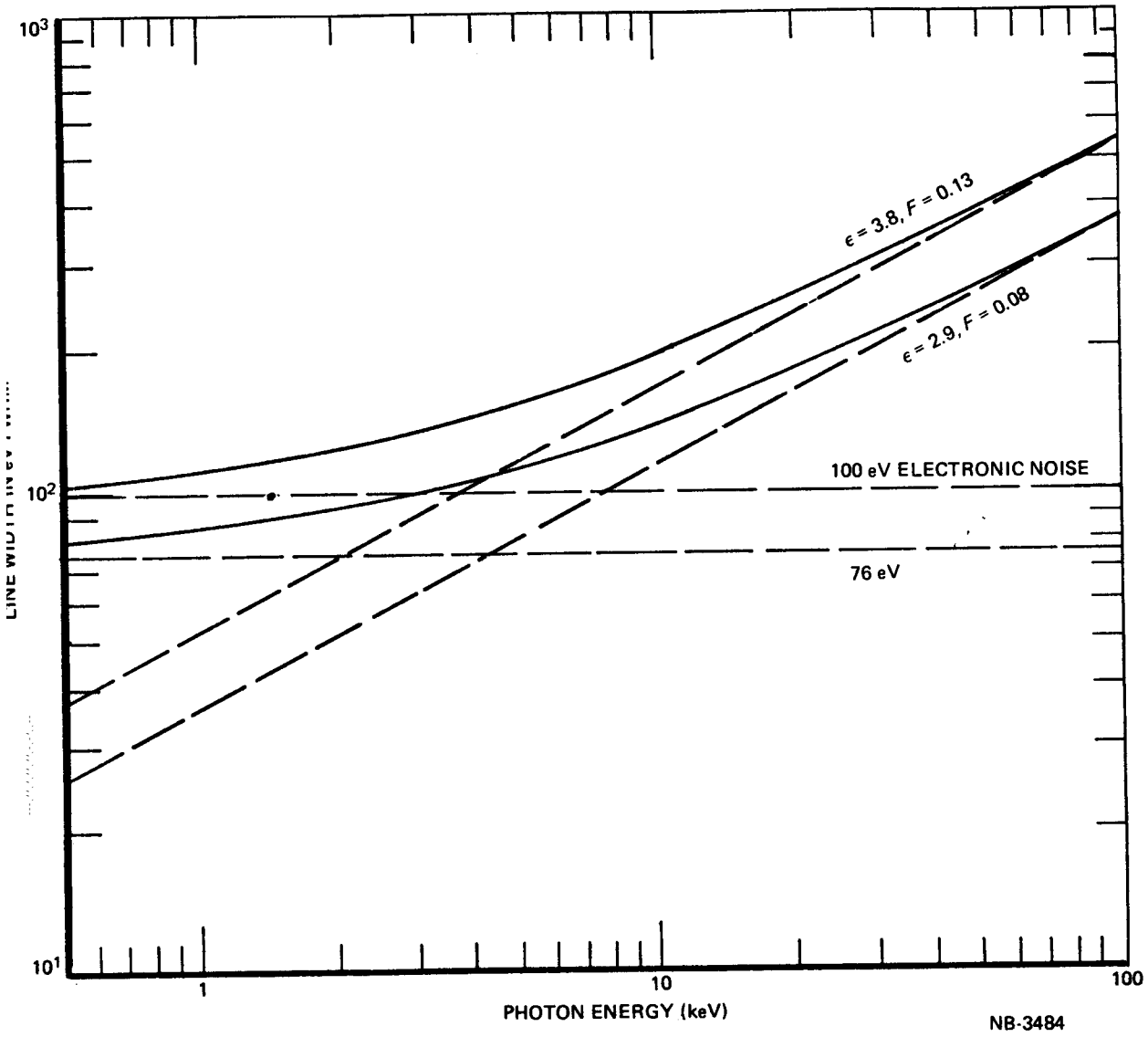


Figure 3—X-Ray Energy Line Width as a Function of Energy for Several Values of Electronic Noise and Fano Factor

5.4 Detector Noise

Leakage current in the detector element and Johnson noise in the detector series resistance can also contribute to system noise and resolution broadening. In integrated X-ray spectrometer systems, it is usually not possible to distinguish unambiguously between series noise sources (for example, the FET series noise) and parallel noise sources such as detector leakage current, feedback resistor, and microphonics. Since the parallel noise predominates at lower frequencies, some indication of the presence of detector current noise or excess feedback noise can be obtained by examining the noise as a function of amplifier passband.

Copyright © 1984 IEEE All Rights Reserved

Copyright The Institute of Electrical and Electronics Engineers, Inc.
Provided by IHS under license with IEEE
No reproduction or networking permitted without license from IHS Not for Resale

5.5 Charge Loss

Loss of free charge carriers because of trapping in the semiconductor crystal can be a significant source of spectral distortion. The peak-width broadening from this effect is proportional to the energy of the X-ray and therefore more pronounced at higher energies. Charge trapping, which is a function of detector bias voltage, frequently results in low energy tails on monoenergetic spectral lines. The effect is, therefore, often more readily apparent in the full width at tenth maximum of the peak height (FWTM) than in the FWHM of the spectral peak. The peak-to-valley ratios of K_α K_β X-ray lines are also quite sensitive to this effect. The FWTM performance of the system is more important than it might appear upon superficial examination. For example, if determining a 10% X-ray fluorescence contribution from one element in the presence of a 90% contribution from the next higher element, the FWTM would be more relevant than the FWHM.

Windows and dead layers, even when not an intimate part of the detector element, contribute to loss of efficiency at low X-ray energies. In addition, charge loss in *partially dead* layers in the portion of the detector adjacent to the entrance window can result in both a loss of full-energy-peak efficiency and in undesirable spectral distortion in the form of a low-energy tail, spurious peaks, and nonlinearity. Since major charge loss problems frequently occur around the outer periphery of the detector active area, these problems tend to be very sensitive to the source-detector geometry employed in the measurement. Consequently, for specification parameters where charge loss is a key variable, it is essential to define the source-detector geometry. This geometry can be conveniently defined in terms of the standard working axis, standard working distance, and standard source diameter. For detectors used in microanalysis applications, the standard source diameter is negligible (a point source).

For the measurements described herein, it is desirable to make a distinction between background and nonideal peak shapes such as asymmetries, tails, spurious peaks, etc. As used herein, the term background will refer only to nonideal spectral response which results from radiation which is not a part of the monoenergetic X-ray line of interest.

5.6 Electronic Stability and Extraneous Noise

The gain stability of the system and excess noise from spurious electrical effects or from microphonics can affect the performance of the system. The FWTM is frequently more sensitive to these problems than the FWHM.

5.7 Count-Rate Effects

5.7.1 Pulse-Shape Considerations and Distortion by Pulse Pile-Up

In order to optimize the signal-to-noise ratio as well as to provide reasonable count-rate capability, restricting both the upper and lower limits of the amplifier passband is necessary. At any given count rate, the width (in time) of the resulting pulse will determine the probability that the preceding or succeeding pulse will be distorted by pulse-on-pulse or pulse-on-tail pile-up. Choice of the type of pulse shaping and the time constants associated with the pulse therefore involves an important compromise between optimum energy resolution at low count rates and the performance of the system at high count rates. Preamplifier noise can frequently be minimized by using relatively long pulse-shaping time constants ([sime]10μs). However, the resulting optimum-shaping time constant for minimum noise can be inconsistent with the count-rate requirements of the user. Consequently, energy resolution specifications should always be accompanied by either the maximum applicable count rate and detailed information on the pulse shape, or a detailed description of the change in FWHM and FWTM as a function of count rate at a specified energy. The latter description of performance is particularly useful in cases where the instrument is to be used in quantitative analysis where changes in resolution with changing count rate would seriously complicate analysis of the resulting data.

The usual shaping time constant number associated with the amplifier is by itself only marginally useful in predicting count-rate capability. The pile-up limitation of the system is primarily determined by the width of the pulse near the baseline. For a given nominal time constant this time interval can vary by a factor of two or more, depending on the

Copyright © 1984 IEEE All Rights Reserved

Copyright The Institute of Electrical and Electronics Engineers, Inc.
Provided by IHS under license with IEEE
No reproduction or networking permitted without license from IHS Not for Resale

type of pulse shaping and the convention used for assigning a time constant value. Although the attainment of low pile-up requires that the characteristic width of the pulse be small compared to the mean interval between pulses, it is also necessary that the pulse return closely to the baseline (average dc level) in a time interval that is small compared to the mean interval between pulses. Many preamplifier systems utilize a design principle referred to as pole-zero (PZ) cancellation to minimize undesirable undershoots. Failure to achieve accurate PZ cancellation can degrade the FWHM and FWTM and can also result in low or high energy tails on spectral peaks, depending on whether an undershoot or overshoot exists. This source of distortion is particularly important at high count rates.

5.7.2 Baseline (dc level) Shifts, Baseline (dc) Restoration, Count-Rate Induced Gain Shifts, and Nonlinearities

A count-rate-induced dc level shift anywhere within the electronic amplifying chain will introduce gain shifts and nonlinearities whenever the dc level exceeds the linear dynamic range of that portion of the signal processing chain. Also, when the limit of the linear dynamic range is approached, statistically induced fluctuations in the dc level can exceed this limit, resulting in peak broadening and other related spectral distortions. In addition, a short-term dc level shift at the output of the amplifier system will produce an equivalent shift in the magnitude of the output voltage pulse presented to the adc of the MCA of single-channel analyzer (SCA), thereby degrading the resolution. Customarily, these problems are reduced by using dc feedback and by using a baseline restorer (BLR) at the output of the amplifying chain. Baseline restoration can also add a noise contribution that depends on the restoration mode and restoration rate (time constant).

Consequently, when specifying resolution, stability, gain shift, linearity, etc, as a function of count rate, stating the following information is essential:

1) The energy for which the performance is specified
2) Details of the pulse shaping
3) Details of restoration mode
4) Details of pile-up rejection

Specifications as a function of count rate shall be obtained at the same operating conditions, for example, same pulse shape, feedback configuration, restoration mode, etc. This requirement is particularly relevant to applications where it is not practical to reoptimize the spectrometer system every time the product of the count rate and the energy changes.

5.7.3 Overload Recovery

Overload pulses produced by high-energy radiation events that exceed the dynamic range of the amplifying equipment can produce undesirable effects such as baseline overshoot or undershoot and system paralysis (dead time). However, since good overload performance may compromise other system characteristics, it should not be emphasized in those applications where overload signals are not a significant problem.

5.8 Detector Material Selection: Germanium Versus Silicon

The two semiconductor detector materials that are presently available for high-resolution X-ray energy spectrometers are germanium and silicon. The relative potential advantages and disadvantages of each are summarized as follows:

Germanium

Advantages

1) Higher atomic number (Z) that results in, better efficiency at high energies.
2) The smaller value of $\in$ reduces the relative importance of noise (see 5.3) and possibly the statistical contribution to the resolution (see 5.2).

Disadvantages

1) Higher efficiency at high energy produces more background problems from high-energy sources.
2) An equal linear thickness for the dead layer (entrance window) corresponds to a much greater efficiency loss at low energy.

Copyright © 1984 IEEE All Rights Reserved

Copyright The Institute of Electrical and Electronics Engineers, Inc.
Provided by IHS under license with IEEE
No reproduction or networking permitted without license from IHS Not for Resale

3) Worse low-energy tailing on low-energy peaks.
4) High efficiency at high-energy increases the probability of amplifier overload.
5) High Z results in increased spectral complication by escape peak problems and a more complex relation between efficiency and energy.
6) Smaller band-gap increases the potential detector leakage current noise problems.

Silicon

Advantages

1) Dead layer effects are smaller.
2) It exhibits relative freedom from escape peak complications in complex spectra.
3) Silicon is less sensitive to high-energy background problems.
4) Silicon can be used at higher temperatures with less detector noise contribution.

Disadvantages

1) Efficiency is lower at high energy (> 30 keV).
2) Higher average energies required to form an electron-hole pair, that is, larger ε.

5.9 Detector Efficiency

The full-energy peak efficiency of a semiconductor X-ray energy spectrometer is energy dependent. It is a function of the physical size and shape of the detector, the presence of windows or dead layers on the detector and its container, charge trapping problems within the detector, the Z of the detector material, and the energy of the K_{abs} edge of the semiconductor.

Typical graphs of efficiency versus energy are illustrated in Fig 4. The low-energy response threshold is established by absorption in the window of the detector entrance surface. In addition, any partially dead layer within the detector near its entrance window may contribute to the drop in efficiency at low energy and may also result in low-energy background counts for peaks at lower energies, that is, a low-energy tall on a monoenergetic X-ray peak. Variations of full-energy peak efficiency as a function of energy are also caused by the sharp change in the absorption coefficient near the K_{abs} edge. Since this sudden increase in cross-section results in a high probability of interaction near the entrance window on the semiconductor, dead or partially dead layers adjacent to the entrance window can cause large drops in the full-energy peak efficiency at energies just above the K_{abs} edge.

Copyright © 1984 IEEE All Rights Reserved

Copyright The Institute of Electrical and Electronics Engineers, Inc.
Provided by IHS under license with IEEE
No reproduction or networking permitted without license from IHS Not for Resale

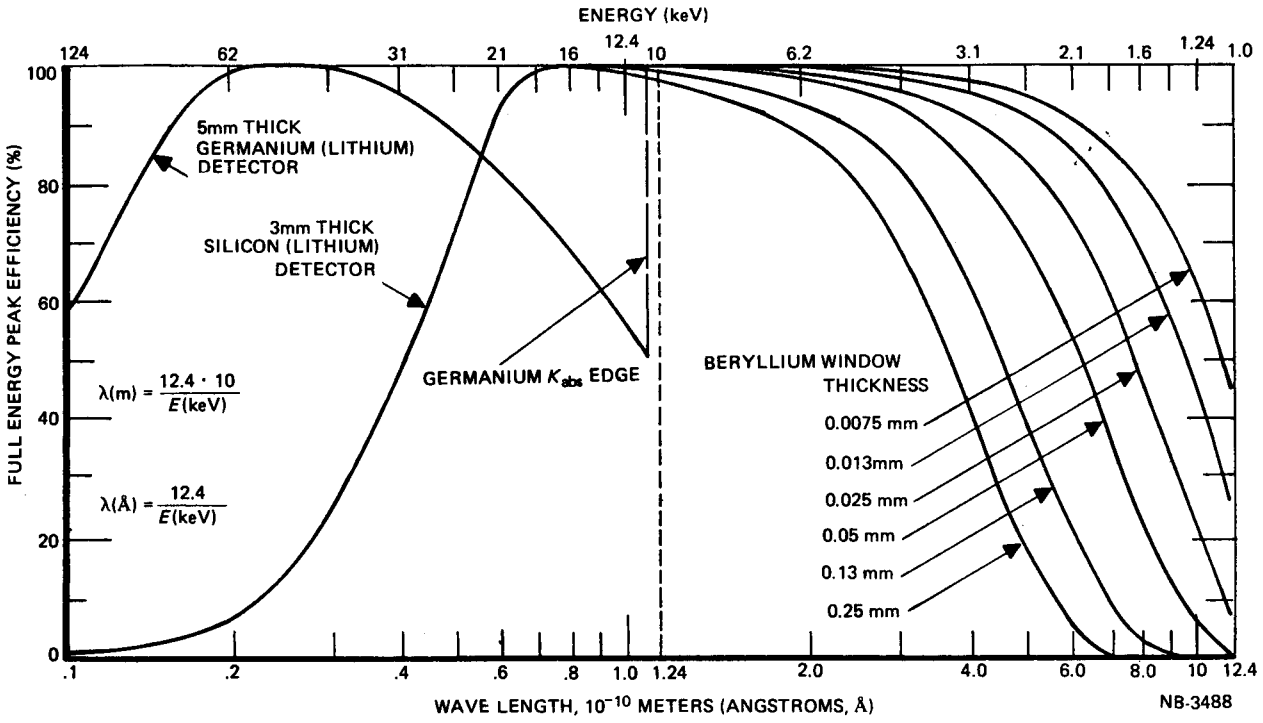


Figure 4—Full Energy Peak Efficiency Versus Energy for Several X-Ray Energy Spectrometers

The drop in efficiency at high energy is established by the sensitive depth and volume of the detector. The efficiency at high energies, as well as the spectral quality (low-energy tailing) can also be affected by the existence of a partially dead layer near the back contact to the sensitive region, by poor charge collection throughout the sensitive region, or by isolated partially dead regions within the sensitive volume.

5.10 Resolution of Adjacent Lines and Line-to-Background Ratio

The question of when two adjacent spectral lines are *resolved* is somewhat subjective since it depends on the particular experimental conditions and performance criteria. For example, when attempting to analyze a line in the presence of a nearby much stronger line, it may be the FWTM of the more intense line that determines whether the lines are *resolved*. When attempting to analyze a line in the presence of a much more intense higher-energy neighbor, it may be the low-energy tailing from the more intense line that establishes the sensitivity and accuracy of the measurement. This standard does not attempt to establish an arbitrary—and possibly misleading—definition to determine if two adjacent lines are resolved. Rather, the approach adopted in this standard is that of defining key characteristics of the spectral response so that the user can interpret the instrument specification with respect to his own needs.

The concept of line-to-background ratio has traditionally been of considerable usefulness to the X-ray analyst. However, the line-to-background ratio in any particular application depends not only on the performance of the X-ray energy analyzer, but also on other factors such as the method of X-ray excitation (for example, electron, heavy ion, secondary X-ray, radioactive source); the character of the fluorescing sample; and geometrical arrangement of the exciting source, target, and detector. Since these latter factors are frequently beyond the control of the X-ray energy spectrometer manufacturer, this standard does not include test procedures for line-to-background ratio determination. However, standards for specifying the characteristic spectrometer parameters such as FWHM, FWTM, peak-to-tail, and peak-to-valley ratios that directly affect the line-to-background ratio have been included, for example, if the FWHM doubles, the line-to-background ratio will decrease to one half, all other factors remaining constant.

Copyright © 1984 IEEE All Rights Reserved

Copyright The Institute of Electrical and Electronics Engineers, Inc.
Provided by IHS under license with IEEE
No reproduction or networking permitted without license from IHS
Not for Resale

5.11 Miscellaneous Other Effects

5.11.1 Microphonics

Microphonic noise generation may be a serious source of resolution broadening. In cryogenic systems, mechanical vibrations of the input circuit components relative to surfaces at different potentials can introduce noise. Such vibrations can be produced by bubbling of liquid nitrogen, turbulence from automatic nitrogen transfer systems, vibration of other equipment in contact with the detector cryostat, and environmental noise. A change of capacitance between the FET gate and the high voltage (detector bias 1000 V) of only 5×10^{-7} pF is sufficient to generate a microphonic signal equivalent to that of a 10 keV X-ray. Since the typical stray capacitances are on the order of 1 pF, mechanical motions (within the frequency pass-band of the shaping amplifier) of approximately one part in $10.^{7}$ are significant. Since most of the vibration problems are at relatively low frequency, much of the microphonic noise is filtered out by the low-frequency roll-off of the amplifier response. Consequently, microphonic problems become more serious at long-shaping time constants. This problem involves the excitation of internal mechanical resonances by internal or external vibrations and is quite complex. Microphonics problems can be studied in a qualitative way by exciting the system with an audio speaker driven by a variable frequency generator. However, because of the wide diversity of detector mechanical configurations available, it would be difficult to establish a standard for microphonics. Nonetheless, the user should be aware of this potential problem.

5.11.2 Secondary Fluorescence

Secondary fluorescence of metal parts of the cryostat, detector, and preamp mount and of the metal electrodes on the detector can cause spectral distortion in the form of spurious peaks in the spectrum.

5.11.3 Liquid Nitrogen Loss Rate

Most semi-conductor X-ray analyzers use liquid nitrogen for cooling the detector and preamplifier. The efficiency of the cryostat design is directly reflected in the liquid nitrogen consumption rate. Excessive liquid nitrogen consumption aggravates microphonics and increases the operating cost, inconvenience, and the chance of accidental warm-up. This performance parameter is usually covered by specifying the capacity of the liquid nitrogen reservoir and the minimum guaranteed holding time.

6. General

6.1 Definition of Semiconductor X-Ray Energy Spectrometer

A semiconductor X-ray energy spectrometer is an instrument which utilizes the proportionality between the energy of an X-ray and the number of free electron-hole pairs created in a semiconductor radiation detector by that X-ray as a means of measuring the energy of the X-ray. In this standard the spectrometer is assumed to consist of the semiconductor detector, preamplifier, means for cooling, encapsulation, required vacuum and mechanical housings, amplifier power supplies, and other required analog electronics. For the purposes of this standard, analog-to-digital data conversion and subsequent data-handling equipment are not considered to be a part of the spectrometer, even though it is recognized that they are an essential ingredient in establishing the total system performance. In addition, sample stages, the X-ray emitter, and means for exciting same (for example, radioactive sources, electron beams, etc) are considered to be ancillary equipment and not part of the spectrometer.

6.2 General Precautions and Specifications

The following general precautions and specifications are relevant to all of the test procedures described herein. Maximum detector bias voltage, rate of bias voltage change, radiation flux ratings, line voltage, maximum detector temperature, and other manufacturers' specification limits should not be exceeded or permanent damage to the

Copyright © 1984 IEEE All Rights Reserved

Copyright The Institute of Electrical and Electronics Engineers, Inc.
Provided by IHS under license with IEEE
No reproduction or networking permitted without license from IHS Not for Resale

instrument may result. The values of the parameters specified should be reproducible within the precision of the measurements after the performance of any one or all of the tests performed. Care should be taken to assure that power-line noise, ground loops, mechanical vibration, and the characteristics of ancillary test equipment do not substantially influence the test results.

Relevant test conditions such as pulse shaping (type and time constants), detector bias, etc, shall be clearly stated. In no case shall performance data that requires change in operating condition or mode be presented as a plotted envelope or table (for example, if energy resolution versus count rate is plotted, all data points must correspond to the same operating conditions). If showing results for several operating modes (for example, time constants) is desired, then these should be shown as a family of curves with operating mode as a parameter.

Since the semiconductor X-ray energy spectrometer user seeks energy and intensity distribution information, specifying system performance in terms of energy spectrum distortion and variations in the system detection efficiency as a function of energy is reasonable. Consequently, many of the performance parameters contained herein are described in terms of deviations from ideal behavior.

In order to establish standardized test procedures that are independent of the various sources of X-rays that might eventually be used with the instrument, readily available radioactive sources have been specified for the test procedures. Whenever possible, isotopes having simple energy spectra have been selected. This is particularly important in resolution versus count-rate tests where multiple lines greatly complicate the interpretation of the data. An attempt has been made to specify standard sources coering the energy range of interest for both silicon and germanium detectors when used with characteristic elemental X-rays. It is recognized that special applications or requirements may necessitate the use of additional X-ray energies to adequately characterize the instrument.

6.3 Simulating the Signal Pulse of a Detector

A pulse from a pulse generator is useful for measuring the electronic noise contribution to the resolution, electronic linearity, gain stability, and also for energy calibrations. In order for all sources of noise, drift, etc, to be sampled by the test pulse, the charge must be injected into the input of the preamplifier as illustrated in Fig 5. The type of pulse generator shown in Fig 5 is frequently referred to as a tail pulse generator. Pulse generators that produce a square pulse are also occasionally used instead of tail pulse generators.

Capacitively coupled test pulses cannot precisely simulate true signal pulses. The exponential decay τ_d shown in Fig 6 corresponds to an uncancelled pole which results in an undershoot at the amplifier output. Pole-zero cancellation of the charge coupling capacitance is not appropriate to this problem, since excess noise at the preamplifier input would result. For a square pulse, droop in the pulse corresponds to a long time constant pole and, in addition, the negative going portions of the pulse will produce a pulse of the wrong polarity in the amplifier and possibly result in undesirable baseline shifts. Consequently, pulse generators should not be used to generate the high and variable count rate required for count-rate-effect measurements. In addition, it is preferable to turn the pulser off during X-ray resolution measurements, particularly if the measurements are performed at high count rates or with long pulse shaping time constants, or both. Some systems, for example, amplifiers with gated BLR, may not tolerate the undershoot from a tail pulse generator or the opposite polarity signal produced by a square pulse generator.

Copyright © 1984 IEEE All Rights Reserved

Copyright The Institute of Electrical and Electronics Engineers, Inc.
Provided by IHS under license with IEEE
No reproduction or networking permitted without license from IHS Not for Resale

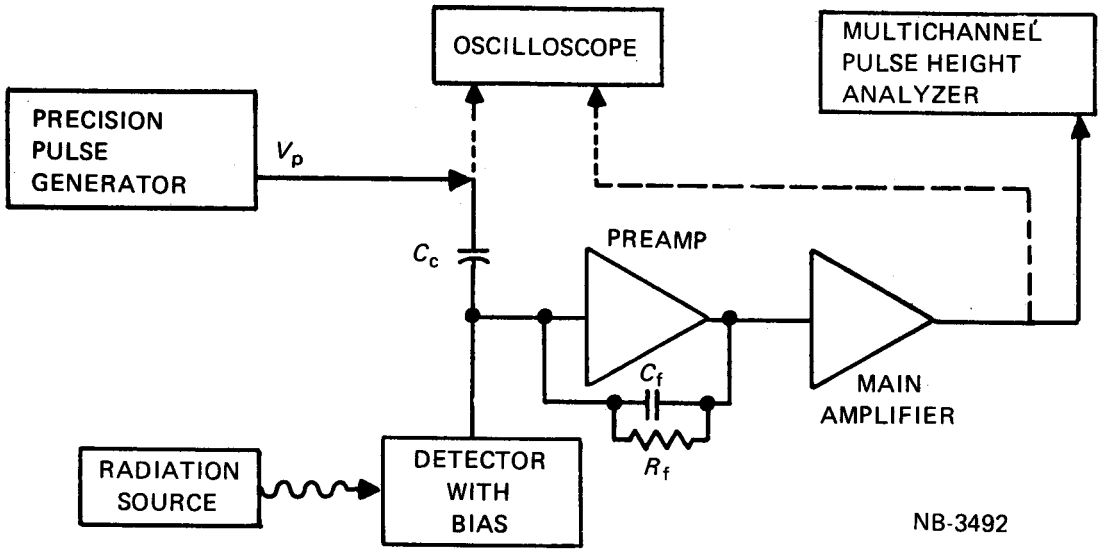


Figure 5—Measurement of Pulse-Height Distribution

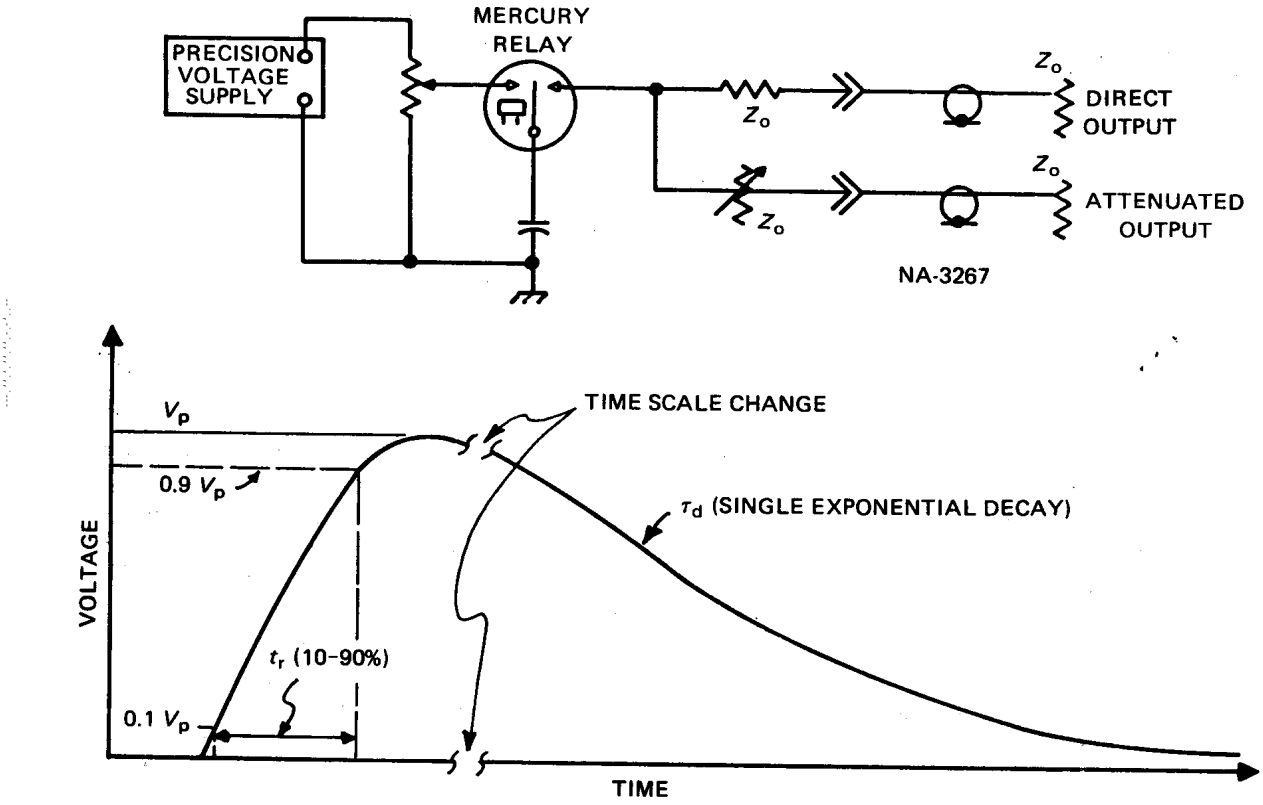


Figure 6—Precision Pulse Generator and Waveform

Copyright © 1984 IEEE All Rights Reserved

Copyright The Institute of Electrical and Electronics Engineers, Inc.
Provided by IHS under license with IEEE
No reproduction or networking permitted without license from IHS
Not for Resale

7. Energy Resolution and Spectral Distortion

7.1 Noise Measurement by Pulse-Height Distribution (Preferred Method)

The electronic and detector noise contribution to the resolution width can be determined by this method only if the instrument is provided with a pulser coupling capacitor (C_c) as shown in Fig 5. The spectrometer is connected to a multichannel analyzer as shown in Fig 5. With all elements of the system operating within their linear range and with the detector at its specified operating voltage, expose the detector to an appropriate X-ray source (for example, 5.9 keV Mn K_α from ^{55}Fe) and accumulate a spectrum. The system gain and pulse amplitude shall be such that the FWHM of the X-ray peak is at least 8 channels and that of the pulser peak is at least 5 channels. (For MCAs with a small number of channels, using a biased amplifier or a digital off-set in the adc following the main amplifier may be necessary to achieve this condition.) Remove the X-ray source and calibrate the pulse generator by setting its output amplitude dial to the appropriate X-ray energy (for example, 5.9 keV) and adjusting the calibration controls until the pulser peak and the X-ray peak have the same peak center (modal) channel. With the source removed, and with the system gain such that the FWHM of the pulser peaks is at least 5 channels, accumulate the 2 peaks corresponding to pulse generator equivalent output energies E_1 and E_2 in channels X_1 and X_2 as shown in Fig 7. The system total noise line width is defined as

$$\Delta_E^T = \left[\frac{E_1 - E_2}{X_1 - X_2}\right]\Delta_N^T \tag{1}$$

where

Δ_N^T = the interpolated number of channels corresponding to the full width of the peak at one half of the maximum height of the peak

The FWTM is defined as

$$\delta_E^T = \left[\frac{E_1 - E_2}{X_1 - X_2}\right]\delta_N^T \tag{2}$$

where

δ_N^T = the number of channels corresponding to the full width of the peak at one tenth of the maximum height of the peak

If the pulse generator is triggered by line frequency, this technique may not detect the presence of noise that is correlated with line frequency. This problem may be avoided by using a pulse generator with an internal trigger that is asynchronous with line frequency.

When stating the total noise line width, complete information on the pulse shaping (including the full-pulse width) shall be given for example, 2 μsec *CR-RC*, or semi-Gaussian with four 2 μsec *CR* integrations and one 2 μsec *RC* differentiation). If baseline restoration (BLR) or gating techniques, or both, are used, the characteristics of the BLR or gating, or both, shall also be stated (see Section 5.).

Copyright © 1984 IEEE All Rights Reserved

Copyright The Institute of Electrical and Electronics Engineers, Inc.
Provided by IHS under license with IEEE
No reproduction or networking permitted without license from IHS Not for Resale

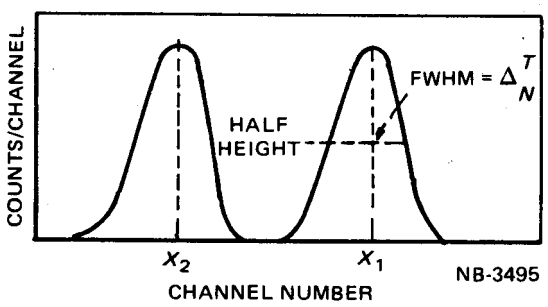


Figure 7—Typical Noise Measurement Pulse-Height Spectrum

7.2 Alternate Techniques For Noise Measurement

7.2.1 Noise Measurement by Oscilloscope and Root-Mean-Square Voltmeter

An alternative method of measuring noise employs the system shown in Fig 8. The root-mean-square (rms) noise voltage level is indicated on an rms voltmeter having a flat-band frequency response extending to at least 10 times the band center frequency of the amplifier pulse-shaping networks. In addition, the amplifier incremental-gain must be constant to below the noise level (a biased amplifier, BLR, or gating can render this measuring technique useless). The same constraints regarding operating conditions and reference specifications outlined in 7.1 apply here also. The pulse generator is calibrated as in 7.1 except that the oscilloscope is used to compare the pulse heights of the source and pulser. A pulse generator pulse equivalent to energy E_p is applied and the resulting amplifier output V_a is measured in the oscilloscope. The pulse generator is switched off and the rms noise voltage e_{no} is read from the voltmeter. The system FWHM noise line width is given by

$$\Delta_E^T = 2.35 \cdot a \cdot e_{no}\left[\frac{E_p}{V_a}\right] \tag{3}$$

where

a = 1.11 for a sine-wave-calibrated average-reading voltmeter and unity for a true rms voltmeter.

The value of $\frac{E_p}{V_a}$ can also be obtained by using a monoenergetic X-ray source of energy E_p.

7.2.2 Noise Approximation from X-Ray Spectral Resolution

The electronic noise contribution to the resolution broadening can also be approximated from the variation of X-ray peak width as a function of energy as given by

$$\Delta_E^T = \sqrt{\left[\frac{\left(\Delta_{E_1}^S\right)^2 \cdot E_2 - \left(\Delta_{E_2}^S\right)^2 \cdot E_1}{(E_2 - E_1)}\right]} \tag{4}$$

where

Δ_E^T = FWHM noise linewidth of Eq 3

$\left(\Delta_{E_1}^S\right)$ = FWHM total linewidth for the peak at energy E_1 (see also 7.4).

Copyright © 1984 IEEE All Rights Reserved

Copyright The Institute of Electrical and Electronics Engineers, Inc.
Provided by IHS under license with IEEE
No reproduction or networking permitted without license from IHS
Not for Resale

Considerable caution needs to be applied in the use of Eq 2, since it is prone to error for the following reasons:

1) The value for Δ^{T}_{E} may be the result of taking a small difference between large numbers, and therefore, the error propagation problem is significant;
2) Eq 2 assumes that the fractional charge loss effects are independent of energy, an assumption that is questionable below 3 keV or over a large energy range;
3) The X-ray peaks are multiplets (for example, $K_{\alpha 1}$, $K_{\alpha 2}$). The separation of these multiplets is a function of energy and whether the peak is a *K*, *L*, or *M* line. This source of variable peak broadening has not been accounted for in Eq 2.

7.3 Noise Linewidth as a Function of Amplifier Time Constants

Information concerning the series and parallel noise contributions can be obtained by plotting noise linewidth as a function of amplifier time constants. In addition, such a plot can give important information regarding the count rate versus energy resolution compromise. To perform this measurement, the method of 7.1 or 7.2 is employed with an amplifier having adjustable shaping time constants. The results are displayed as a plot of noise linewidth as a function of pulse-shaping time constants (with other possible variables such as BLR as a parameter).

7.4 X-Ray Linewidth Measurements by Pulse Height Distribution

7.4.1 X-Ray Sources

The following radioactive sources are recommended for specification of energy resolution:

(a)	^{55}Fe	5.9 keV-Mn K_{α} ($K_{\alpha 1}$ – 5.898, $K_{\alpha 2}$ – 5.887)
(b)	^{109}Cd	22.162 ($K_{\alpha 1}$) and 21.988 ($K_{\alpha 2}$) keV Ag *K* X-rays and 88 keV gamma ray
(c)	^{57}Co	6.4 Fe K_{α} ($K_{\alpha 1}$ – 6.403, $K_{\alpha 2}$ – 6.390) and 14.4, 122, and 136 keV gamma rays (not recommended for count-rate effect measurements)

If resolution is specified at only one energy, ^{55}Fe is the preferred source. The 5.9 keV Mn X-ray represents a reasonable compromise between amplifier noise broadening and other detector resolution broadening effects. The lines above 30 keV are relevant mostly to germanium detectors: To prevent spectral distortion from backscattered radiation, the source backing thickness and *Z* should be kept as small as possible.

Copyright © 1984 IEEE All Rights Reserved

Copyright The Institute of Electrical and Electronics Engineers, Inc.
Provided by IHS under license with IEEE
No reproduction or networking permitted without license from IHS Not for Resale

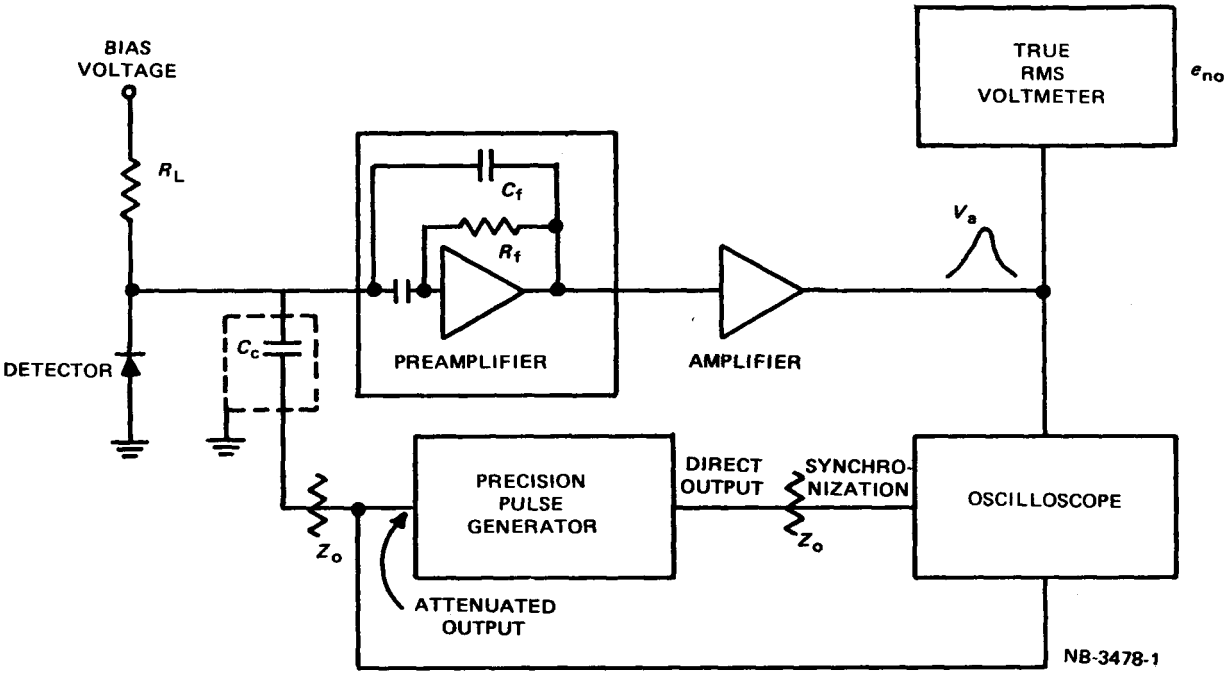


Figure 8—Noise Measurement by Oscilloscope and True Root-Mean-Square Voltmeter

If lower-energy lines are desired, they may be obtained by secondary fluorescence of a target such as the standard glass described in Section 12..

In case a secondary fluorescent target is used as a source of X-rays for resolution measurements, the background from the continuum should be subtracted before determining N_x (the counts in channel X). A suitable technique for background subtraction is described in 12.1 of this standard, and in 4.1 of both ANSI/IEEE Std 325-1971 [3] and IEC Publication 430 (1973) [6].

7.4.2 Spectral Resolution

These tests are carried out using the system of Fig 5 and one of the radiation sources listed in 7.4.1. The source is located on the standard working axis of the detector at the standard working distance. The active diameter of the source must not significantly exceed the standard working diameter. For those cases where the source is a true characteristic X-ray, the location of the centers of the K_α and K_β peaks can be used to obtain the calibration

$$S = \left[\frac{E_1 - E_2}{X_1 - X_2}\right] \tag{5}$$

For other cases, or if the K_α and K_β are not sufficiently well resolved, the pulser technique of 7.1 may be used to obtain calibration. The results should be expressed as the FWHM and FWTM. The FWHM is obtained from the relation

$$\Delta_E^S = \left[\frac{E_1 - E_2}{X_1 - X_2}\right]\Delta_N^S \tag{6}$$

Copyright © 1984 IEEE All Rights Reserved

Copyright The Institute of Electrical and Electronics Engineers, Inc.
Provided by IHS under license with IEEE
No reproduction or networking permitted without license from IHS
Not for Resale

where[3]

Δ_N^S = full width (in interpolated fractional channels[3] of the peak at one half of its maximum amplitude

The FWTM is given by

$$\delta_E^S = \left[\frac{E_1 - E_2}{X_1 - X_2}\right]\delta_N^S \tag{7}$$

where

Δ_N^S = full width in (fractional channels) of peak at one tenth of its maximum amplitude

For a Gaussian peak,

$$\delta_N^S = 1.78\left(\Delta_N^S\right), \text{ thus } \delta_E^S = 1.78\left(\Delta_E^S\right)$$

The FWHM must be at least 10 channels with a minimum of 40 000 counts in the peak center (modal) channel. In reporting information on spectral resolution the following shall be noted:

a) Incident X-ray source and energy
b) Count rate at which measurement was taken
c) Detector-source geometry (standard working distance and standard source diameter)
d) Detailed description of detector and its collimator (shape, area, depth, silicon or germanium, etc)
e) Detector operating bias
f) System noise linewidth under the same operating conditions
g) Amplifier pulse-shaping parameters (including the full pulse width and BLR parameters)

Another set of parameters of interest are those contributions to the detector linewidth caused by all factors other than electrical noise (for example, statistical and charge collection problems). These quantities are found by subtracting the noise linewidth contributions in quadrature according to the relationships

$$\Delta_E^O = \sqrt{\left(\Delta_E^S\right)^2 - \left(\Delta_E^T\right)^2} \tag{8}$$

and

$$\delta_E^O = \sqrt{\left(\delta_E^S\right)^2 - \left(\delta_E^T\right)^2} \tag{9}$$

It is relevant to point out that the resolution limit set by statistical considerations alone is given by

$$\lim\left[\Delta_E^O\right] = 2.35\sqrt{F\varepsilon E} \tag{10}$$

[3] Method of interpolation shall be given by manufacturer.

Copyright © 1984 IEEE All Rights Reserved

Copyright The Institute of Electrical and Electronics Engineers, Inc.
Provided by IHS under license with IEEE
No reproduction or networking permitted without license from IHS Not for Resale

where

Δ_E^O = FWHM linewidth in units of energy

E = X-ray energy
ε = average energy to form an electron-hole pair and
F = Fano Factor

The value of the Fano Factor is not accurately established at the present time for either silicon or germanium. Existing experimental data establish only a probable upper limit for F; however, $F = 0.1$ is commonly employed as a useful estimate of F.

7.5 Peak-to-Valley and Peak-to-Tail Ratios

Peak-to-valley ratios (7.5.1) for two closely spaced peaks (for example, the K_α and K_β of *Mn* from ^{55}Fe) and peak-to-tail ratios (7.5.2) can be very sensitive indicators of spectraldistortions caused by a variety of factors ranging from charge collection problems in the detector (or its partially dead windows) to baseline in stability and other related count-rate effects in the electronics. Peak-to-tail ratios can also be sensitive indicators of the detector system's line-to-background ratio capability.

When quoting peak-to-valley or peak-to-tail ratios complete details of the measurement conditions, including source-detector geometry (standard working distance and standard source diameter) amplifier time constant settings, input count rate, and any other major variables that would significantly affect the measurement shall be clearly stated. The system parameter adjustments used for these specifications should be consistent with those used for specification of other performance parameters, such as FWHM, etc.

7.5.1 Peak-to-Valley Ratio

The peak-to-valley ratio between two specified peaks is defined as the ratio of the height of the larger peak to the height in the minimum of the valley between the two peaks.

Specifications of peak-to-valley ratios should be based on sufficient statistical information (that is, number of counts per channel in the valley) to assure a maximum statistical probable error of less than 5% in the peak-to-valley ratio.

7.5.2 Peak-to-Tail Ratio

This test consists of placing the active side of a ^{55}Fe source normal to and centered on the standard working axis and located at the standard working distance, adjusting gains so that at least 10 channels appear across the FWHM, and counting until N_p counts (20 000 minimum) are accumulated in the peak center channel (modal channel) at 5.9 keV. The number of counts in each of the groups of 5 contiguous channels centered around the energies of 5.4 keV, 4.5 keV, and 1 keV, respectively, are averaged to give values C_1, C_2, and C_3, respectively.

The peak-to-tail ratios P_1, P_2, and P_3 are calculated from

$$P_1 = \frac{N_p}{C_1} \qquad P_2 = \frac{N_p}{C_2} \qquad \text{and} \qquad P_3 = \frac{N_p}{C_3} \tag{11}$$

Reduction of the peak-to-tail ratio may result from deterioration in system performance from contributions due to backscattering from the surroundings or source backing, high count rates, system noise (ground loops, ac noise, etc), improper equipment settings (misadjustment in PZ cancellation networks, non-optimum shaping times, etc) or the presence of other radiation sources in the vicinity. Background from origins other than the ^{55}Fe source must be negligible in order to make this measurement meaningful.

Copyright © 1984 IEEE All Rights Reserved

Copyright The Institute of Electrical and Electronics Engineers, Inc.
Provided by IHS under license with IEEE
No reproduction or networking permitted without license from IHS Not for Resale

This method for the determination of the peak-to-tail ratio can yield misleading results if there are other radionuclide impurities in the source that contribute to events in the tail. Errors resulting from impurities in the source can be detected by remeasuring the peak-to-tail ratio with an absorber placed between the ^{55}Fe source and the detector.

8. Pulse Height Linearity

8.1 System X-Ray Linearity by Pulse-Height Analyzer Method (Preferred Method)

This technique measures the combined integral nonlinearity of the detector system and the pulse-height analyzer. To determine the integral linearity of any component of the instrument chain, the effect of the other components must be measured and subtracted.

With the arrangement shown in Fig 5 the detector is exposed to a series of characteristic X-ray lines spanning the energy region of interest. Normally, a minimum of ten lines, more or less uniformly spaced over the region of interest is required for a good linearity check. These lines may be generated by secondary excitation induced with X-rays, gamma rays, or charged particles. The lowest energy line should be less than 10% and the maximum energy line greater than 90% of full-scale energy range of interest.

Care should be exercised to use only lines whose characteristic energy is accurately established (for example, unresolved multiplets that result in significant resolution broadening should be avoided whenever possible).

If these lines are generated sequentially rather than simultaneously, care should be exercised to ensure that the counting rate is low and comparable; otherwise, count-rate-induced gain shifts may be mistakenly interpreted as a pulse-height linearity problem. Also care should be taken that equipment gain drifts are not mistakenly interpreted as nonlinearities. The most reliable method is to generate all of the lines simultaneously.

Integral nonlinearity (*INL*) is defined as the maximum deviation from linearity expressed as a percentage of the specified maximum linear output. When characterized by a single unqualified number, *INL* shall not exceed that number anywhere within the specified operation range of the instrument and shall be determined under the same conditions (instrument settings, etc) used to specify resolution performance. The *INL* may be obtained from the previously described X-ray spectrum by plottingpeak center (modal) channel number for each peak versus the X-ray energy of that peak as shown in Fig 9.

The ideal response curve is a straight line corresponding to a linear regression least squares fit to the data points with the same statistical weight for all measurements. The *INL* in percent is then defined by

$$INL = 100\left(\frac{\Delta E_{\mathrm{Max}}}{E_{\mathrm{F}}}\right) \tag{12}$$

where

ΔE_{Max} = maximum deviation (in energy units) between the measured and the ideal response
E_{F} = energy corresponding to the full scale of the energy range of interest

8.2 Integral Linearity by the Bridge Method

This measurement (supplementary method) is described in detail in 5.1 of ANSI/IEEE Std 301-1976 [2], and in Section 21 of IEC Publication 340 (1979)[5]. It can be utilized only with detector systems that incorporate a pulser coupling capacitor as described in 7.1.

Copyright © 1984 IEEE All Rights Reserved

Copyright The Institute of Electrical and Electronics Engineers, Inc.
Provided by IHS under license with IEEE
No reproduction or networking permitted without license from IHS Not for Resale

9. Count Rate Effects

9.1 Experimental Arrangement

Because most instruments which utilize gated baseline restoration do not tolerate the reverse polarity part of the pulse of a tail pulse generator or a square pulse generator, techniques which rely on a pulse generator to measure count-rate effects are frequently not useful for X-ray spectrometers

The experimental arrangement for using a radioactive source to measure count-rate effects on spectral distortion is shown in Fig 10. The ^{55}Fe source shown in Fig 10 is located on the working axis of the detector, and the source-to-detector distance is varied to change the counting rate. Generally, it is preferable that the radioactive source be sufficiently intense that the maximum desired counting rate is obtained at a source-to-detector spacing not less than the standard working distance. If the source-to-detector spacing is too small, spectral distortions from edge effects in the detector may be misinterpreted as count-rate-induced distortions. All extraneous scattering materials must be kept well away from the space between or adjacent to the source and detector to eliminate spectral distortion by Compton scattered photons, or by secondary fluorescence X-rays. In general, it is preferable to use an X-ray source that does not produce any high-energy events that would overload the amplifier. It is essential that the input stages of the adc be dc coupled.

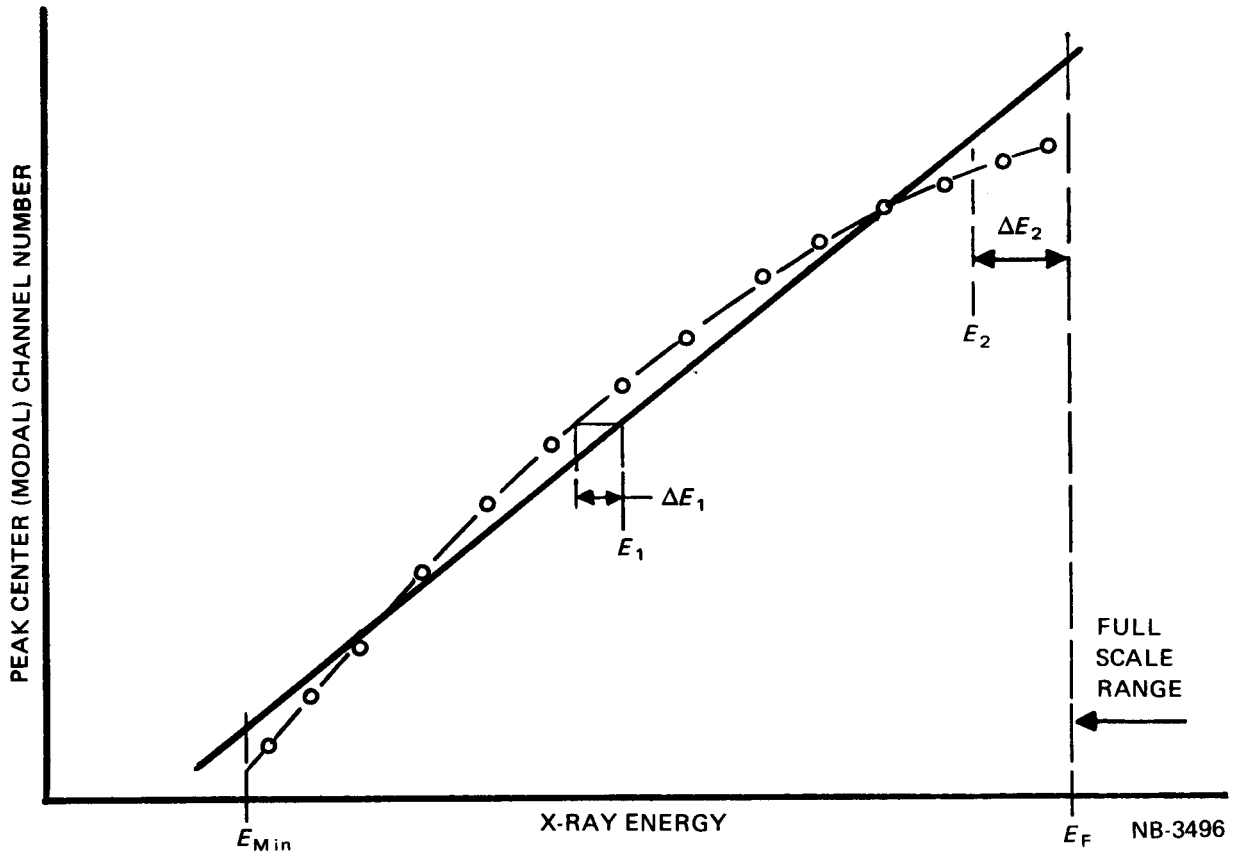


Figure 9—Measurement and Display of Linearity

Copyright © 1984 IEEE All Rights Reserved

Copyright The Institute of Electrical and Electronics Engineers, Inc.
Provided by IHS under license with IEEE
No reproduction or networking permitted without license from IHS
Not for Resale

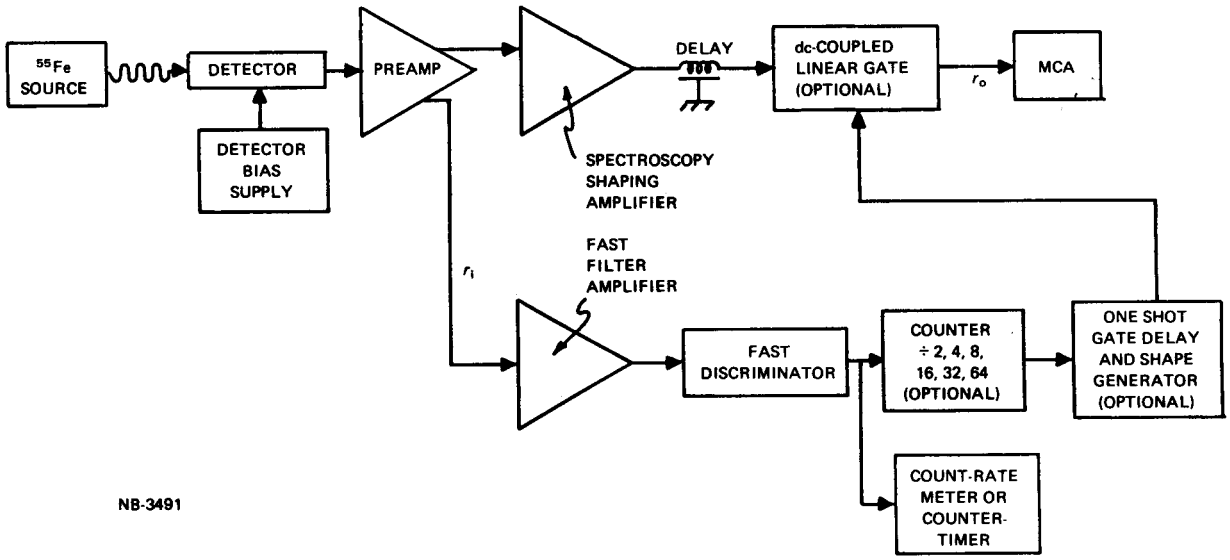


Figure 10—Experimental Arrangement Using Multichannel Analyzer to Measure Spectral Distortion Resulting from Counting Rate Effects

The equivalent input count rate (r_i) is measured by the fast amplifier, discriminator, and count-rate meter. In preamplifiers which utilize pulsed feedback, the r_i shown in Fig 10 does not represent the true input rate: to obtain the true input rate in this case, a correction must be made for the dead time caused by the gated-off periods. In some cases, this correction may be very significant. The fast filter amplifier chain must have a bandpass sufficient to ensure negligible counting losses, or an accurate correction for the counting loss from pile-up must be applied. A good first-order correction is given by the relation

$$r_o = r_1(e)\exp(-r_1 t_w) \tag{13}$$

where

r_o = unpiled-up output data rate (per second)
r_i = input data rate (per second)
t_w = width of the pulse (in seconds) at the baseline established by the discriminator threshold level

If the arrangement shown in Fig 10 is operated in the ungated mode (that is, with the gate bypassed) the observed count rate effects will include the contributions from the MCA. The contribution from the MCA (and gate) alone can be approximated in the following way:

Set the scaler overflow output to divide-by-one condition and the delay and the one-shot period long enough to gate the entire amplifier output pulse through the linear gate. Adjust the ^{55}Fe source position to produce the maximum desired counting rate. Vary the counting rate into the MCA by switching the scaler overflow output to ÷ 2, ÷ 4, ÷ 8, ÷ 16, ÷ 32, etc. The resulting shifts inresolution and peak shape can be attributed to the MCA and linear gate. The contribution from the linear gate can be minimized by using a good quality dc coupled linear gate.

Because of the derandomizing effect of the scaler, this technique will tend to underestimate the count-rate effects in the MCA at low and medium count rates.

Copyright © 1984 IEEE All Rights Reserved

Copyright The Institute of Electrical and Electronics Engineers, Inc.
Provided by IHS under license with IEEE
No reproduction or networking permitted without license from IHS
Not for Resale

The main problems with count-rate effect measurements are the following:

1) The difficulty of isolating the contribution of any one component of the detector-preamplifier-amplifier-MCA system; and
2) The dependence of count-rate performance on many factors, such as signal energy, preamplifier noise, and amplifier shaping time constants.

It is therefore necessary, in specifying the system performance, that all the relative operating conditions be clearly stated, and that the system parameters are selected so as to approximate the conditions under which the system will be used. When investigating count rate performance, it is imperative that the PZ cancellation networks and baseline restorers be properly adjusted.

When specifying system performance, the following shall be stated:

1) Whether the results include the MCA effects
2) Energy range
3) Amplifier shaping time constants, including BLR setting and pile-up rejection
4) Low count-rate resolution
5) Energy at which the amplifier overloads
6) Radiation source and energy used for random signal source (preferred source is ^{55}Fe)

When specifying performance as a function of counting rate, the counting rate specified shall always be the counting rate at the input (detector) of the spectrometer. The output counting rate that corresponds to this input counting rate shall also be stated.

9.2 Pulse-Height Distribution Peak Shift

The peak location (centroid) of a pulse-height distribution may exhibit dependence on total counting rate. The experimental setup Shown in Fig 10 provides a means to measure pulse-height shift as a function of average counting rate for random pulse spacing in time. The counting rate is varied by adjusting the spacing between the radiation source and the detector and is measured with a count-rate meter. The Mn K_α peak should be set at 90% of the maximum specified linear output of the system. The counting rate should then be varied over the entire range of interest, and the shift of the *Mn* K_α peak centroid plotted as a function of total input count rate.

9.3 Spectral Resolution and Line Shape Versus Count Rate

The setup shown in Fig 10 is also used for this measurement. The FWHM, FWTM, and peak-to-tail of the Mn K_α pulse height distribution are measured for each of several counting rates over the range of interest and tabulated or plotted as a function of input count rate. The Mn K_α peak should be set as specified in 9.2.

9.4 Counting Losses

At high counting rates, pulse pile-up will cause a loss of counts from the peak as well as spectral distortion. In addition, systems which use gating techniques to eliminate spectral distortion or to effect pulsed feedback to the preamplifier will exhibit dead times during the gate-closed periods. All systems are paralyzable; that is, at some level of input count rate, the output count rate actually decreases with increasing input rate. Fig 11 illustrates this effect.

Either the arrangement shown in Fig 10 or that of Fig 12 may be used for this measurement. If the arrangement of Fig 10 is used, the count-rate meter should be replaced with a counter-timer, and the gain should be adjusted as in 9.2. If the arrangement in Fig 12 is used, the window widths in the fast single channel analyzers should be set at 6 times the FWHM, and the center of the window should correspond to the peak center (modal point of the peak) at low count rate. The arrangement shown in Fig 12 can be used only under situations where the pulse-height distribution peak shift with

Copyright © 1984 IEEE All Rights Reserved

--`,,`-`-`,,`,,`,`,,`---
Copyright The Institute of Electrical and Electronics Engineers, Inc.
Provided by IHS under license with IEEE
No reproduction or networking permitted without license from IHS Not for Resale

counting rate will not shift the peak out of the window of the SCA. The fast filter amplifier chain must have a bandpass sufficient to ensure negligible counting losses, although a small calculated dead-time loss correction for the fast filter amplifier chain may be required.

The count rate is increased by decreasing the source-to-detector distance, and the counting rate of the analyzed pulses in the X-ray peak is plotted as a function of total count rate in the fast filter amplifier chain as shown in Fig 13. The results of Fig 11 can be derived from those of Fig 13. Counting loss effects which are attributable to the MCA may be measured by disabling the coincidence gate input shown in Fig 10 (as described in 9.1).

The arrangements of Fig 10 or 12 can also be used to verify dead-time corrections.

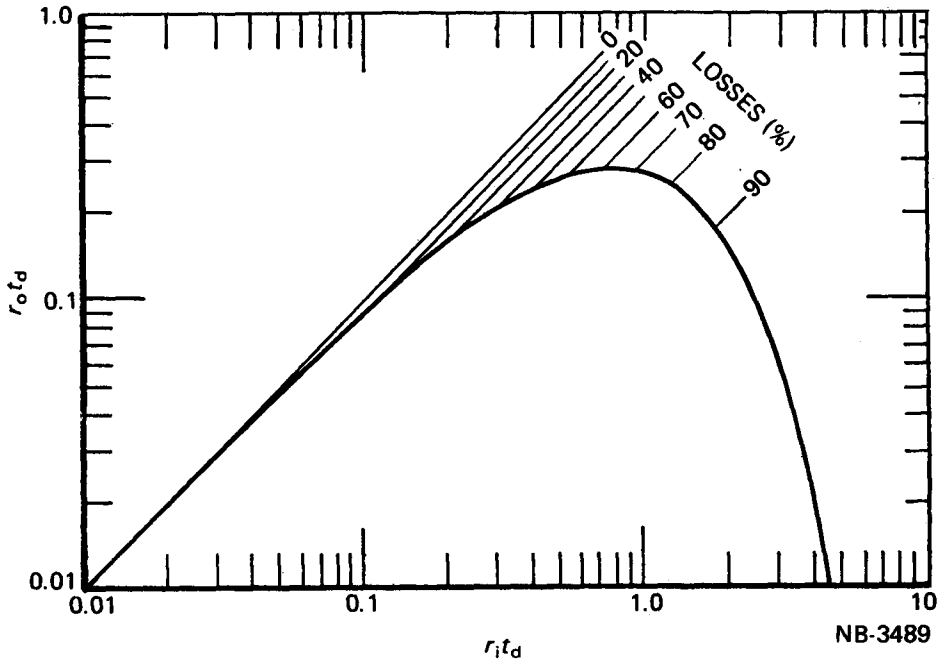


Figure 11—Output Rate r_o Versus r_i for a Paralyzable System with a Deadtime t_d

Copyright © 1984 IEEE All Rights Reserved

Copyright The Institute of Electrical and Electronics Engineers, Inc.
Provided by IHS under license with IEEE
No reproduction or networking permitted without license from IHS
Not for Resale

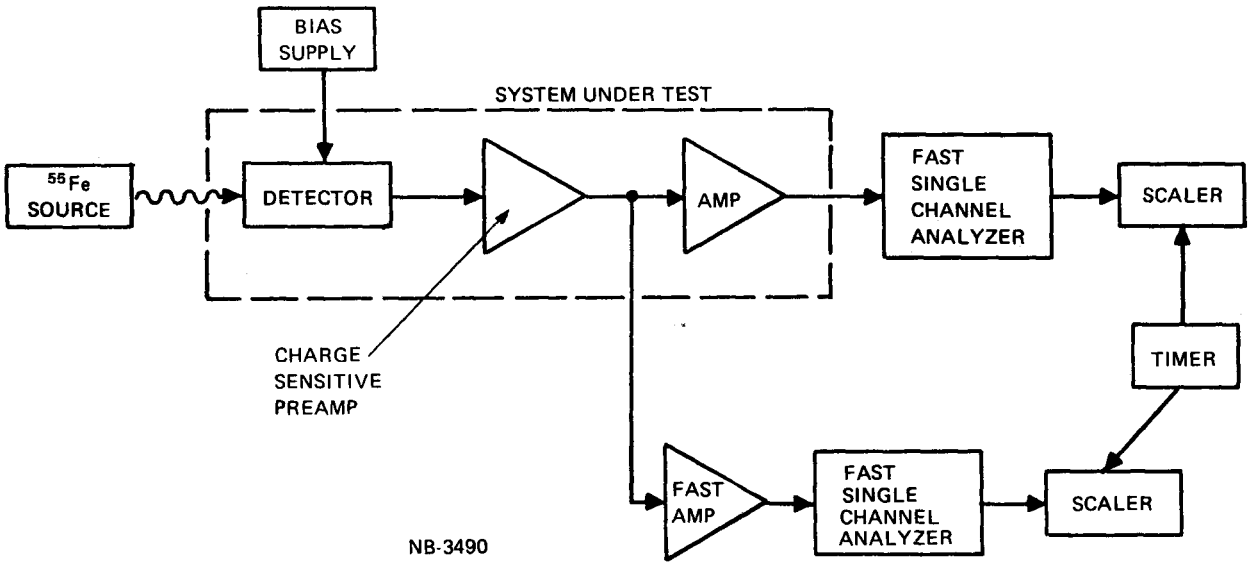


Figure 12—Experimental Arrangement Using Single-Channel Analyzers to Measure Counting Losses

Copyright © 1984 IEEE All Rights Reserved

Copyright The Institute of Electrical and Electronics Engineers, Inc.
Provided by IHS under license with IEEE
No reproduction or networking permitted without license from IHS
Not for Resale

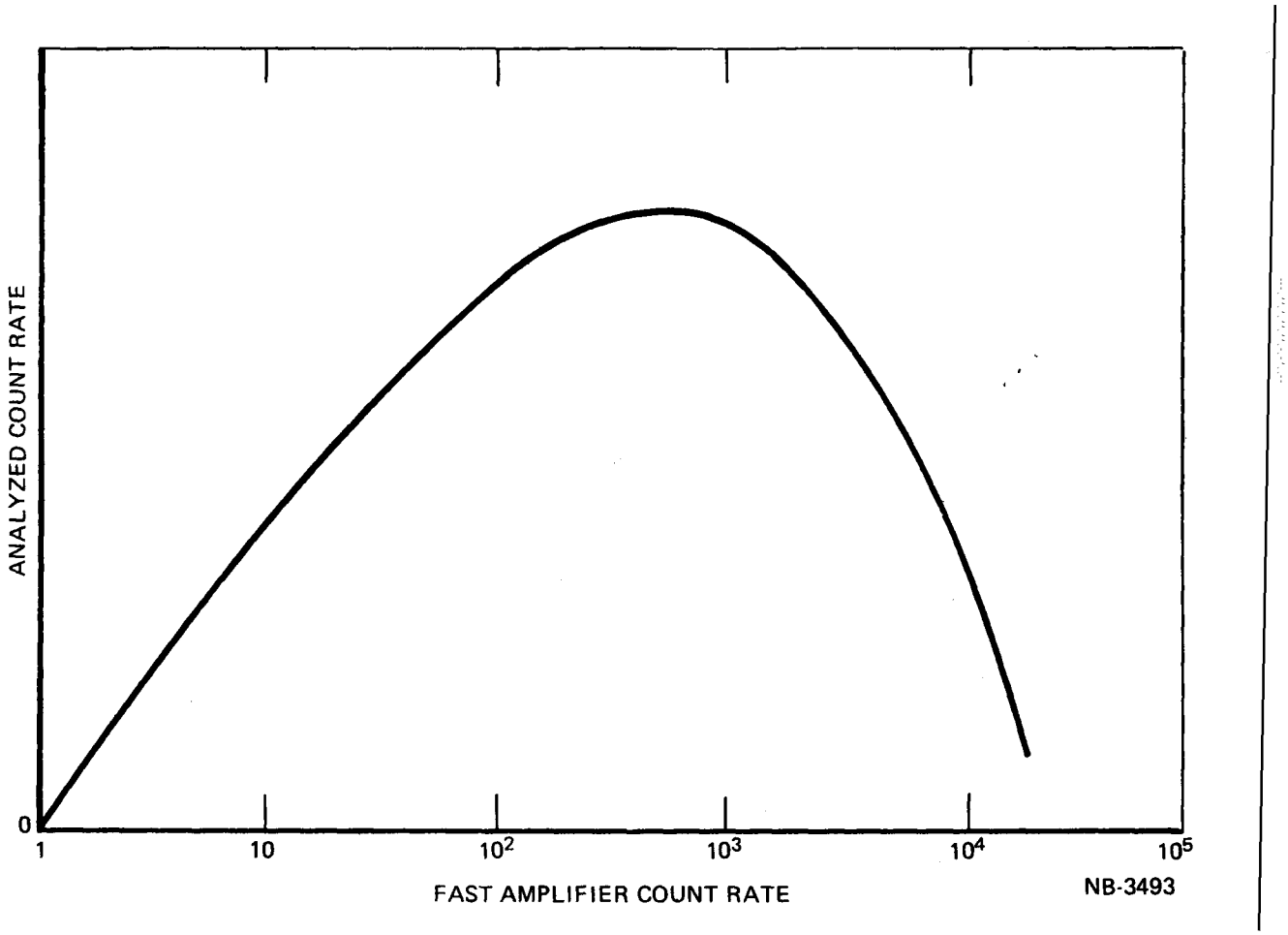


Figure 13—Analyzed Count Rate in Mn K_α and K_β Peaks as a Function of the Count Rate From a Fast Amplifier

10. Overload Effects

10.1 General

The behavior of an amplifier to an input pulse that drives the amplifier far into the overload region depends on many factors. The order in which different sections of the amplifier overload as the input amplitude is increased may depend on the gain control and time constant settings. All of the gain control settings and pulse shape parameters shall be stated when the overload recovery time is specified; otherwise, the specification shall apply for all gain and filter networks combinations available in the system. Amplifiers having adjustable PZ cancellation and baseline restoration networks must be properly adjusted before overload tests are performed.

10.2 Amplifier Gain Recovery Time

A system is defined as having recovered from overload when the output waveform returns to and remains within a band about the baseline of 1% of the maximum specified output voltage, and when the gain for small signals has returned to normal. After an overload pulse, the output waveform of some amplifiers returns to the baseline sooner than

Copyright © 1984 IEEE All Rights Reserved

Copyright The Institute of Electrical and Electronics Engineers, Inc.
Provided by IHS under license with IEEE
No reproduction or networking permitted without license from IHS
Not for Resale

the gain returns to normal. Return-to-normal gain may usually be judged by the reappearance of full noise or small signal response on the oscilloscope trace. The test arrangement shown in Fig 5 permits a quick measurement of recovery time after an overloading pulse. If the pulse generator is replaced with a sine-wave generator, working at low signal level, the reappearance of the sine wave can be used instead of the noise. An example of such overload behavior is illustrated in Fig 14. Note that the small sinusoidal signal on the trace reappears when the amplifier gain has returned to normal. The waveform returns to the baseline very quickly after the overload pulse, but the gain does not recover until much later. Oscilloscope overload must be avoided. Amplifier gain recovery time shall be stated for overload factors of 10, 100, and 1000 at all relevant time-constant and gain settings.

11. Pulse Height Stability

11.1 Line Voltage Variations

The test setup is identical with that shown in Fig 5 except that the line voltage is variable to all parts of the system except the precision pulse generator, multichannel analyzer, and oscilloscope. A pulse generator peak or a peak from a monoenergetic X-ray line (that is, ^{55}Fe), or both, may be used to measure stability. Set the line voltage at its nominal value and adjust the amplifier output so that the peak center (modal) channel of the peak N_l is at 90% of full scale on the MCA. Observe the maximum deviation of N_l as the line voltage is varied over a range of 88–110% of the nominal operating voltage while all other conditions are maintained constant. This variation is often expressed in percentage for a given line voltage change and is obtained by the relation

$$S_{\mathrm{L}} = 100\frac{\Delta N_l}{N_l} \tag{14}$$

A similar test may be performed with a biased amplifier in the system. In this case, the pulse generator and gains should be adjusted to give 90% of maximum rated output voltage from the biased amplifier at the desired gain and bias level setting. Spectra should be obtained at 88% and 110% of nominal line voltage. Output pulse height stability S_{L} (pulse height variation over a +10%, -12% line voltage range) is given in percent by

$$S_{\mathrm{L}} = 100\frac{\Delta N_l}{N_l + G_{\mathrm{B}}N_{\mathrm{B}}} \tag{15}$$

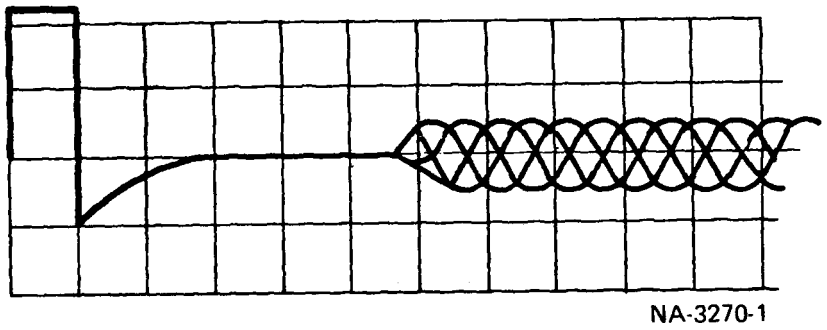


Figure 14—Example of Gain Recovery After Overloading Pulse

Copyright © 1984 IEEE All Rights Reserved

Copyright The Institute of Electrical and Electronics Engineers, Inc.
Provided by IHS under license with IEEE
No reproduction or networking permitted without license from IHS
Not for Resale

where

ΔN_l = number of channels between the peak center (modal) channels of the peaks
G_B = gain of the biased amplifier in eV/channel
N_B = equivalent number of channels suppressed by the biased amplifier

Measurement of the effect of the MCA on pulse height stability can be accomplished by repeating the above with variable line voltage to the MCA only.

11.2 Temperature Effects

For this test, the system shown in Fig 5 (except for the pulse generator, MCA, and oscilloscope) is placed in an environmental test chamber. The maximum change in pulse height produced by incremental changes of the ambient air temperature, with other conditions maintained constant, is the temperature coefficient of pulse height; for example, 0.01% per degree Kelvin.

In amplifiers with dc coupling, pulse height shifts can be caused by either gain changes or dc level shifts. When applicable, temperature induced pulse-height changes in both gain and dc level shall be measured and specified. When specifying the temperature coefficient of pulse height, the range over which the specification applies must be clearly stated. The measurements shall be made over a specified temperature range and taken at no greater than 10° K increments. The specified temperature coefficient must be valid for all increments within the specified temperature range. Care should be taken not to damage the system by operating outside of the manufacturer recommended operating temperature range.

11.3 Gain Stability

The test setup is identical with that shown in Fig 5 and 11.1. Gain variations can be determined by observing the peak center (modal) channel shift in the MCA. Test conditions should be maintained constant and the maximum gain variations noted over an extended period of time which shall be stated.

12. Efficiency[4]

The efficiency of a semiconductor detector at a given photon energy is a function of a number of variables including the area, shape, and depth of the active region, the presence of collimators, and the absorption in windows (or dead layers) between the source of X-rays and the active region. In addition, the presence of nearby extraneous scattering material can also bias the accuracy of efficiency measurement. In specifying the efficiency of the detector, it is also essential that the active area be specified.

Since the periphery of the sensitive region is usually a charge collection problem area, many semiconductor X-ray spectrometers are constructed with internal collimation. Any description or specification of the active area of the detector should unambiguously specify the dimensions, shape, *Z*, and location of collimators. Other regions of low electric field in the device may also cause spectral distortions; therefore, in specifying the sensitive depth of the detector, the thickness of any nondepleted material shall be clearly stated.

[4]See also Stone, R. E., Walter, F. J., Blackburn, D. H., Pella, P., and Kraner, H. W. A Standard Technique for Measuring Window Absorption and Other Efficiency Losses in Semiconductor Energy-Dispersive X-Ray Spectrometry, *Journal of X-Ray Spectrometry*, vol 10, no 2, 1981 (pp 91–96)[lB].

Copyright © 1984 IEEE All Rights Reserved

Copyright The Institute of Electrical and Electronics Engineers, Inc.
Provided by IHS under license with IEEE
No reproduction or networking permitted without license from IHS Not for Resale

12.1 Window Attenuation Measurements with Glass Fluorescent Source (Preferred Method for Instruments Intended for Use Below 5 keV)

In this measurement, the ratios of the relative intensities of fluoresced X-rays from a standard glass with composition as in Table 1 are used to quantify the attenuation in the cryostat window and the detector dead layer.

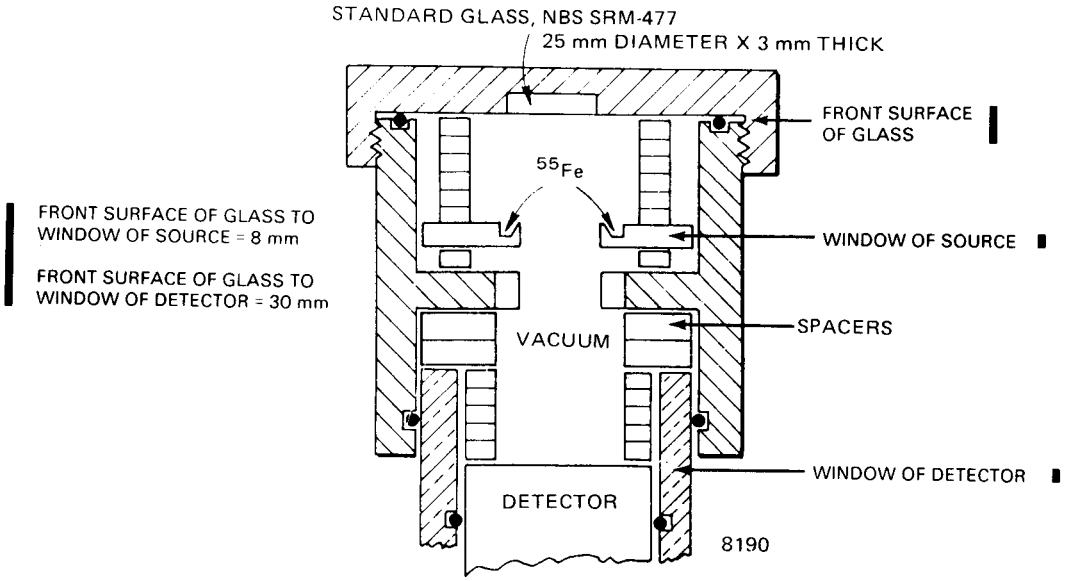
The standard glass shall be excited by ^{55}Fe as illustrated in Fig 15. The resulting X-ray spectrum obtained with the arrangement of Fig 5 is used to characterize the window attenuation.

Since the relative intensities of the fluorescent X-ray lines incident on the detector window are affected by absorption in the glass target, this measurement is sensitive to the source-glass-detector geometry. The geometric arrangement shown in Fig 9 has been selected to minimize the effect of small variations in the dimensions, while still maintaining a reasonable counting rate. With the geometry shown in Fig 15 and a $1.9 \cdot 10^9$ Bq (50 mCi) ^{55}Fe source, the data shown in Fig 16 (with 400 000 counts in the *Mn* K_α peak) can be obtained in about 5 h. Any portion of the structure, except the glass target, that could emit interfering secondary X-rays must be shielded from the detector with plastic. Plastics containing catalysts or fillers that emit interfering X-rays must be avoided.

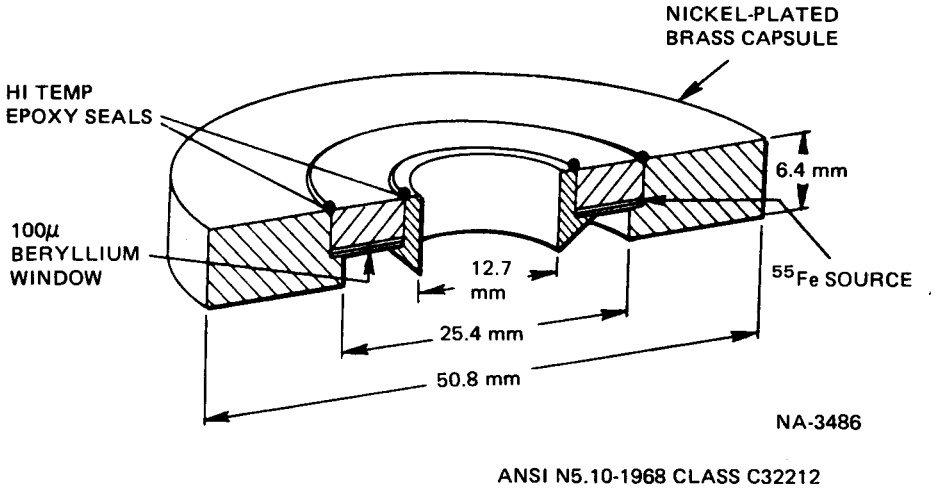
The typical spectrum shown in Fig 16(a) was obtained using an Si (Li) detector in a cryostat with an 8 μm thick beryllium window. Figure 16(b) shows the effect of interposing an additional 124 μm thick beryllium absorber. The indices of interest are the intensities of the low-energy lines relative to the intensity of the coherently backscattered *Mn* K_α line.

Copyright © 1984 IEEE All Rights Reserved

Copyright The Institute of Electrical and Electronics Engineers, Inc.
Provided by IHS under license with IEEE
No reproduction or networking permitted without license from IHS Not for Resale



(a) Apparatus for Window Thickness Measurements



(b) Annular ^{55}Fe X-Ray Source

Figure 15—Fluorescent X-Ray Source Assembly for Window Thickness Measurements

The nominal composition of NBS Standard Glass SRM 477 is shown in Table 1.

Fluorescence of the standard glass with a ^{55}Fe source produces the prominent lines shown in Table 2.

Copyright © 1984 IEEE All Rights Reserved

Copyright The Institute of Electrical and Electronics Engineers, Inc.
Provided by IHS under license with IEEE
No reproduction or networking permitted without license from IHS
Not for Resale

Fig 16 (a) clearly shows Ba, Ca, Si, and Mg lines, while the *Zn-L* line is barely detectable above the background.

The window index W_E at a given energy E is defined by the relationship

$$W_E = \frac{A_E}{A_{\mathrm{Mn}}} \tag{16}$$

where

A_E = total number of counts in the peak at energy E
A_{Mn} = intensity of the backscattered *Mn-K* line

Table 1—
Composition of NBS SRM 477*

(Weight percent calculated from batch charge composition)			
SiO_2	42.5	MgO	20.0
BaO	2.0	ZnO	20.0
CaO	1.5	B_2O_s	10.0
Li_2O	4.0		

*US National Bureau of Standards Standard Reference Material 477

Table 2—
Characteristic X-Ray Lines from the Standard Glass Fluoresced by ^{55}Fe Source*

Mn, K_α	5.90 keV (coherent backscatter)
Ba, $L_{\alpha 1}$	4.47, $L_{\alpha 2}$ – 4.45, $L_{\beta 1}$ – 4.83, $L_{\beta 2}$ – 5.16, L_γ – 5.53
Ca,K_α	3.69, K_β – 4.01, L – 0.34
Si, K_α	1.74, K_β – 1.83
Mg, K_α	1.25, K_β – 1.30
Zn, L_α	1.01, L_β – 1.03
O, K_α	0.523
B, K_α	0.185 keV

*The ^{55}Fe source used in these studies was a New England Nuclear Model NER-461A. (See Fig 15 and also Stone, R E., Walter, F.J., Blackburn, D.H., Pella, P., and Kraner, H.W. A Standard Technique for Measuring Window Absorption and Other Efficiency Losses in Semiconductor Energy Dispersive X-Ray Spectrometry, *Journal of X-Ray Spectrometry*, vol 10, no 2, 1981, pp 91-96[1B].)

The procedure for determining A from a spectrum such as Fig 16 is described at the end of this section.

Frequently, a single value for W_E will adequately characterize the drop-in efficiency at low energies. However, additional useful information about the origin of the window attenuations can sometimes be obtained by comparing values of W_E at several energies. When an instrument is characterized by a single W_E it should correspond to the lowest energy line which will provide data of reliable statistical accuracy. Lines with line-to-background ratios of less than 3 should normally not be used. If the propagation of statistical errors in the determination of W_E exceeds ± 3% at the 90% confidence level, then the probable error (90% confidence limit) in the value of W_E shall also be specified.

Copyright © 1984 IEEE All Rights Reserved

Copyright The Institute of Electrical and Electronics Engineers, Inc.
Provided by IHS under license with IEEE
No reproduction or networking permitted without license from IHS
Not for Resale

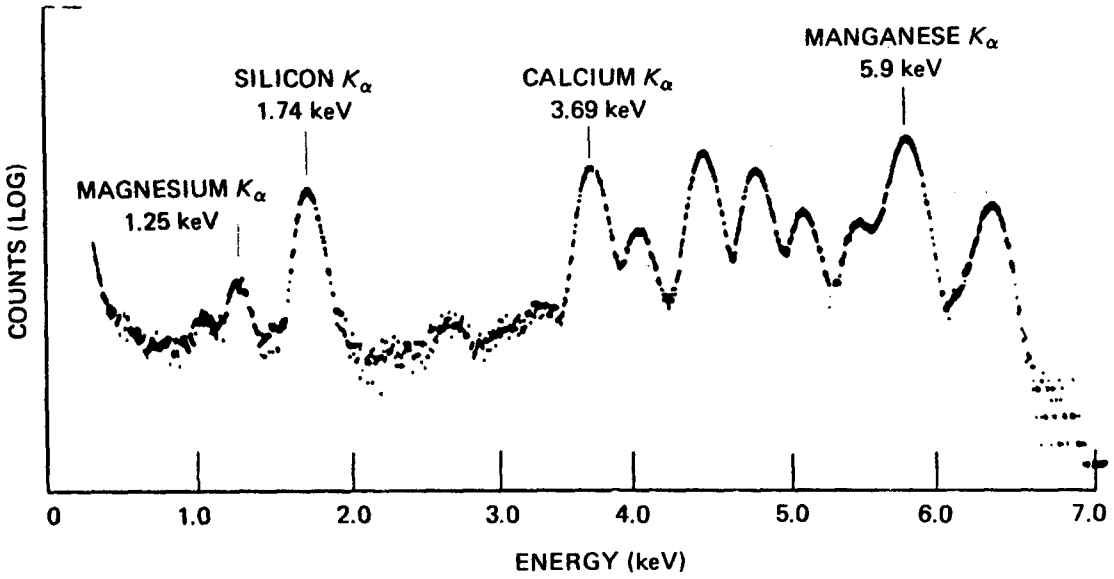
Typical values of W_E for the example shown in Fig 16 are illustrated in Fig 17 which is included here only for the purpose of illustrating the sensitivity of this technique.

The procedures described in this section are also useful for *windowless* detectors where the vacuum-tigh barrier between the detector and source of X-rays is removed during operation. In this case, care must be exercised to ensure that either the detector or preamplifier, or both, are not damaged by poor quality of the vacuum in the vicinity of the X-ray fluorescent source.

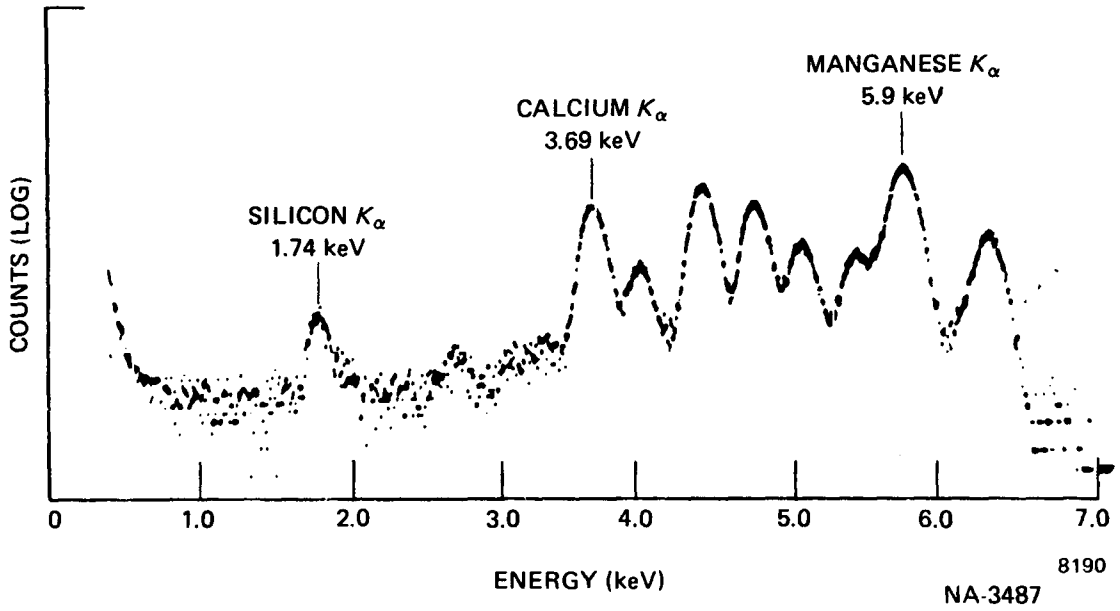
The method for peak area and spectral background subtraction has been chosen for its simplicity and ease of computation, although in certain circumstances, such as in the presence of seriously. distorted spectral peaks, the method could yield misleading results. For the analyses described below, a spectral peak must be at least 6 channels wide at half-maximum and the total number of counts within the FWHM shall be at least 10 000. If computer fitting of the data is used, the 10 000 counts minimum need not apply, provided the result as calculated by computer is accurate to within ± 3% (90% confidence level). Pulse-height spectral data should be plotted as the log of the number of counts N_x in the channel x versus channel number x. On this plot, background under the X-ray peaks is determined by a linear fit to the average backgrounds on the upper and lower energy sides of the peaks of interest (see line B_1–B_2 of Fig 18). The counts within the peaks are determined as those above this background line up to clearly defined minima between adjoining peaks. Background and peak definitions are shown in Fig 18. Peaks not clearly defined should not be used, and the peak-to-valley ratio should not be less than 10.

Copyright © 1984 IEEE All Rights Reserved

Copyright The Institute of Electrical and Electronics Engineers, Inc.
Provided by IHS under license with IEEE
No reproduction or networking permitted without license from IHS Not for Resale



(a) Spectrum Obtained with an 8 μm Beryllium Window

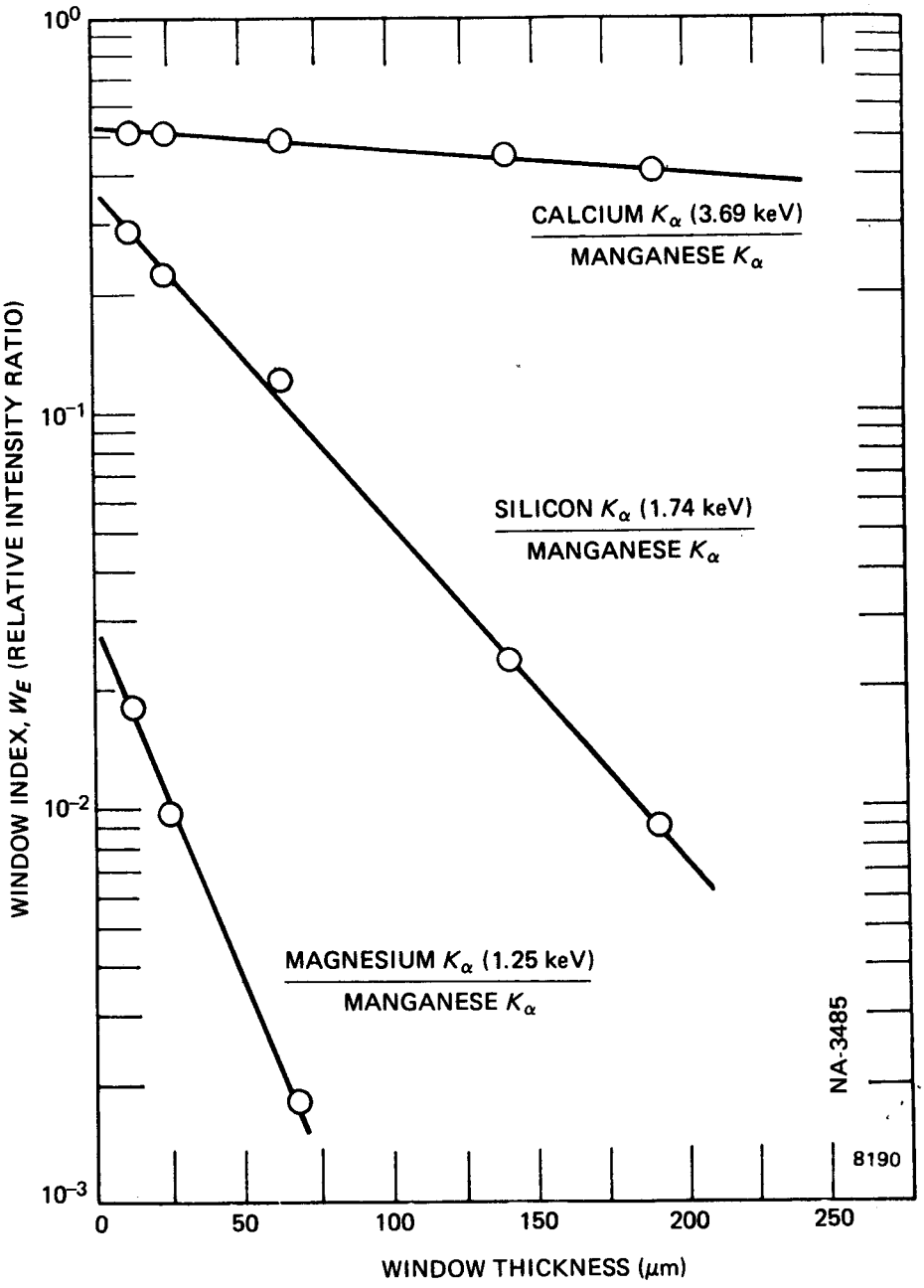


(b) Spectrum Obtained with a 132 μm Beryllium Window

Figure 16—Typical Si Detector Spectra for ^{55}Fe-Excited Standard Glass

Copyright © 1984 IEEE All Rights Reserved

Copyright The Institute of Electrical and Electronics Engineers, Inc.
Provided by IHS under license with IEEE
No reproduction or networking permitted without license from IHS
Not for Resale



Data from STONE, R. E., WALTER, F. J., BLACKBURN, D. H. and PELLA, P. Standard Techniques for Measuring Window Absorption and Other Efficiency Losses in Semiconductor X-Ray Energy Spectrometers, Proceedings, Energy Dispersive X-Ray Spectrometry, National Bureau of Standards, Gaithersburg, Maryland 20760, April 23-25, 1979, *National Bureau of Standards Special Publication 604*, June 1981, pp 61-70.

Figure 17—Typical Behavior of the Window Index, W_E, as a Function of Window Thickness at Several Energies*

Copyright © 1984 IEEE All Rights Reserved

Copyright The Institute of Electrical and Electronics Engineers, Inc.
Provided by IHS under license with IEEE
No reproduction or networking permitted without license from IHS Not for Resale

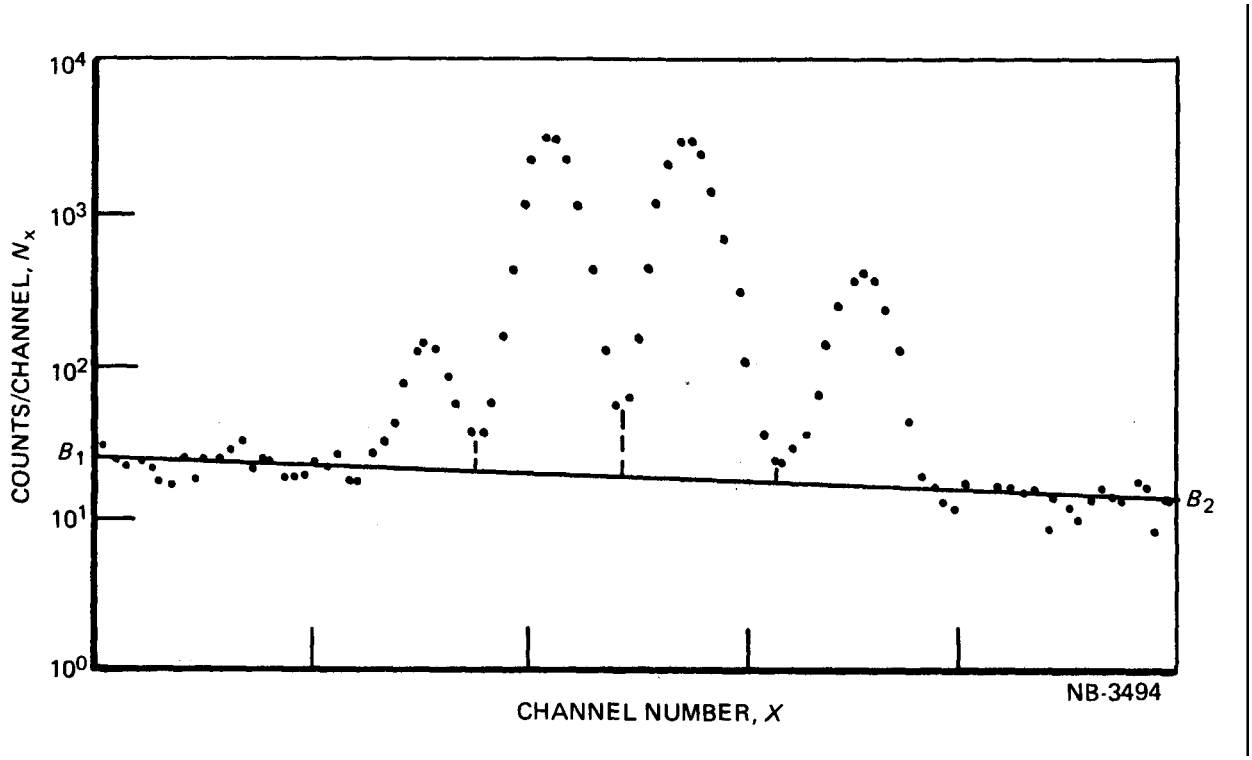


Figure 18—Background Subtraction and Peak Area Measurements

12.2 Window Attenuation Measurement with Radioactive Sources

Some detectors not intended for operation below 6 keV may have a dead layer or window that is too thick to allow use of the techniques described in 12.1. In this case, a similar procedure which employs a radioactive source with two or more lines whose relative intensities are well known can be used to specify W_E. The intensity of the higher energy line is the denominator in Eq 8. The detector must be thick enough to totally absorb the higher energy X-ray. For this measurement, the glass target and the ^{55}Fe source are replaced by the appropriate radioactive source located on the working axis of the detector at the specified working distance.

For example, if ^{109}Cd is used, the detector sensitive region must be thick enough to totally absorb the 88 keV X-rays and the window thickness index is given by the ratio of A_{22} over A_{88}. For cases where the source has more than two characteristic lines care must be taken to clearly specify which two lines are used to determine W_E. Care must be taken also to ensure that self-absorption in the source and its housing is negligible.

Typical sources that are useful for this measurement are listed in Table 3.

Copyright © 1984 IEEE All Rights Reserved

Copyright The Institute of Electrical and Electronics Engineers, Inc.
Provided by IHS under license with IEEE
No reproduction or networking permitted without license from IHS Not for Resale

Table 3—
Radioactive Sources for Characterizing Window Thickness*

Radioactive Source	Energy (keV)	Probability Per Decay
^{57}Co	6.4	0.494 ± 0.015
	14.4	0.0954 ± 0.0013
	122.0	0.866 ± 0.019
	136.0	0.1061 ± 0.0018
^{109}Cd	22.1	0.842 ± 0.028
	88.0	0.0373 ± 0.0006
^{133}Ba	30.9	0.969 ± 0.020
	35.0	0.226 ± 0.006
	53.2	0.0217 ± 0.0004
	81.0	0.335 ± 0.005
	161.0†	0.0062 ± 0.0004
^{125}I	27.2	0.398 ± 0.014
	27.5	0.742 ± 0.025
	31.0‡	0.258 ± 0.010
	35.5	0.0667 ± 0.0022

*Data from A *Handbook of Radioactivity Measurements Procedure*, NCRP Report No 58, Nov 1, 1978. National Council on Radiation Protection and Measurements, 7910 Woodmont Avenue, Washington, DC 20014.
†Avoid the use of the 161 keV line of ^{133}Ba as a reference peak because of interference from sum peaks.
‡Average of K_β lines.

12.3 High Energy Efficiency Measurements

The drop-in efficiency at high energies is a function of detector sensitive depth and diameter, the Z of the semiconductor, and the details of the collimation. The easiest way to measure most of these parameters is by direct physical measurement before the system is assembled. In addition, the sensitive depth of the detector element can usually be estimated by the capacitance-voltage characteristics of the diode before it is assembled with the preamp. Some verification of these parameters may be obtained by measuring the absolute efficiency at one or more appropriate energies. Additional information may sometimes also be obtained by measuring the efficiency as a function of source-to-detector spacing. In these types of measurement, care should be taken to avoid the presence of extraneous scattering material that might scatter photons into the detector.

Copyright © 1984 IEEE All Rights Reserved

Copyright The Institute of Electrical and Electronics Engineers, Inc.
Provided by IHS under license with IEEE
No reproduction or networking permitted without license from IHS Not for Resale

Table 4—Standard Sources for Efficiency Measurements[5]

Source	Half-Life	Energy (keV)	Probability Per Decay	
^{55}Fe	2.7 yr	5.89	0.082	± 0.007
(*Mn*-K_α,K_β		5.90	0.163	± 0.012
		6.49	0.033	± 0.003
^{125}I	60.1 d	27.2	0.398	± 0.014
		27.5	0.742	± 0.025
		31.0	0.258	± 0.010
		35.5	0.066 7	± 0.002 2
^{109}Cd	464 d	22.1	0.842	± 0.028
		24.9	0.060 4	± 0.002 3
		88.0	0.037 3	± 0.000 6
^{152}Eu	13.3 yr	121.8	0.283 8	± 0.002 3
		244.7	0.075 1	± 0.000 7
		344.3	0.265 8	± 0.001 9
		411.1	0.02233	± 0.000 13
		444.0	0.031 79	± 0.000 45
		779.0	0.129 6	± 0.000 7
		964.0	0.145 2	± 0.000 6
		1086.0	0.101 6	± 0.000 5
		1112.0	0.1356	± 0.0006
		1408.0	0.208 5	± 0.000 9
^{60}Co	5.27 yr	1173.2	0.99900	± 0.00020
		1332.5	0.999 824	± .000 005
^{133}Ba	10.74 yr	30.9	0.969	± 0.020
		35.0	0.226	± 0.006
		53.2	0.021 7	± 0.000 4
		81.0	0.335	± 0.005
		276.4	0.070 9	± 0.001 3
		302.9	0.184 0	± 0.002 0
		356.0	0.621	± 0.007
		383.9	0.089 1	± 0.001 0

[5]Ibid..

Copyright © 1984 IEEE All Rights Reserved

Copyright The Institute of Electrical and Electronics Engineers, Inc.
Provided by IHS under license with IEEE
No reproduction or networking permitted without license from IHS
Not for Resale

In attempting to interpret these types of measurements, it is essential to know the relevant dimensions, positioning, and *Z* of the collimators since the collimators may not be totally effective at high energies.

If the detector element is not totally depleted, then its efficiency will be a function of detector bias voltage for X-ray energies which are not totally absorbed by the sensitive region.

Some available standard sources which are useful for absolute efficiency measurements are listed in Table 4.

13. Bibliography

[1B] STONE, R.E., WALTER, F.J., BLACKBURN, D.H., PELLA, P., and KRANER, H.W. A Standard Technique for Measuring Window Absorption and Other Efficiency Losses in Semiconductor Energy Dispersive X-Ray Spectrometry, *Journal of X-Ray Spectrometry*, vol 10, no 2, 1981.

Copyright © 1984 IEEE All Rights Reserved

Copyright The Institute of Electrical and Electronics Engineers, Inc.
Provided by IHS under license with IEEE
No reproduction or networking permitted without license from IHS Not for Resale